

Superconductors with charge- and spin-density waves: theory and experiment

(Review Article)

A. M. Gabovich and A. I. Voitenko

*Crystal Physics Department, Institute of Physics, National Academy of Sciences
46, Nauki Ave., 03650, Kiev-39, Ukraine
E-mail: collphen@marion.iop.kiev.ua;*

Received July 6, 1999, revised December 22, 1999

The properties of existing superconductors with electron spectrum instabilities, namely charge-density waves (CDW's) and spin-density waves (SDW's), are reviewed. In such substances the superconducting gap exists over the whole Fermi surface, whereas the dielectric gap emerges only on its nested sections. In particular, CDW superconductors include layered dichalcogenides, NbSe_3 , compounds with the *A15* and *C15* structures, etc. There is a lot of evidence that high- T_c oxides also belong to this group of materials. SDW superconductors include, e.g., URu_2Si_2 and related heavy-fermion compounds, Cr–Re alloys and organic superconductors. The theoretical description given in this review is based mostly on the Bilbro–McMillan model of the partially dielectrized metal. Various thermodynamic and electrodynamic properties are calculated in the framework of this model. The main subject of the review is the nonstationary Josephson effect in tunnel junctions involving CDW or SDW superconductors. A new effect of symmetry breaking in symmetrical tunnel junctions is predicted by the authors. A comparison with experiment is given.

PACS: 74.20.-z, 74.25.-q, 74.70.-b, 74.72.-h, 74.50.+r, 71.45.Lr, 75.30.Fv

Contents

Introduction	420
1. Experimentally observed partially dielectrized superconductors	422
1.1. CDW superconductors	422
1.2. SDW superconductors	426
2. Implications for high- T_c oxides	429
3. Formulation of the theoretical approach	432
3.1. Generic Hamiltonians of the DW superconductors and the Dyson–Gor'kov equations	434
4. Theoretical description of thermodynamic properties and comparison with experiment	436
4.1. Superconducting and dielectric gaps	436
4.2. Heat capacity	437
4.3. Impurity effects	438
5. Theoretical description of electrodynamic properties and comparison with experiment. Upper critical magnetic field	439
6. Josephson effect	441
6.1. Green's functions	441
6.2. Tunnel currents	441
6.3. Stationary Josephson effect (critical current)	442
6.4. Nonstationary Josephson effect (theory)	442
6.5. Discussion and comparison with experiment	444
6.5.1. CDW superconductors	444
6.5.2. SDW superconductors	446
Conclusions	447
Acknowledgments	447
Bibliography	447

Introduction

The concept of the dielectric structural transition due to the electron-phonon interaction (commonly called the Peierls transition) has its roots in the thirties, but it became wide-spread after the publication of the book [1]. At the same time, Fröhlich [2] considered a possible sliding of the collective state involving electrons and lattice displacements in the one-dimensional (1D) metal as a manifestation of superconductivity. The emergent concomitant energy gap was identified by him with a superconducting gap rather than with the dielectric Peierls gap, as had to be done. It is remarkable that the very concept of the electron spectrum energy gap in the superconducting state had been put forth by Bardeen almost simultaneously with Fröhlich and even before the microscopic Bardeen—Cooper—Schrieffer (BCS) theory was constructed [3].

Fröhlich's point of view [2] was revived after the sensational discovery of the giant conductivity peak in the organic salt TTF-TCNQ [4]. However, the coherent transport phenomena appropriate to the quasi-1D substances appeared to be a manifestation of a quite different collective state: charge-density waves (CDW's) [5]. Their coherent properties now constitute a separate and interesting branch of solid-state science, but they lie beyond the scope of our review and will be touched upon hereafter only in specific cases where necessary.

As to the superconductivity itself, it was explained in the BCS theory on the basis of the Cooper pairing concept and was later shown by Gor'kov to be described by a peculiar type of broken-symmetry state, specifically, a state with off-diagonal long-range order (ODLRO) [6]. Such a state is characterized by the two-particle density matrix

$$\hat{\rho} = \langle \Psi_{\alpha'}^+(r_1') \Psi_{\alpha}^+(r_1) \Psi_{\alpha}(r) \Psi_{\alpha'}(r') \rangle, \quad (1)$$

where Ψ (Ψ^+) is the annihilation (creation) field operator; $\langle \dots \rangle$ means the thermodynamical averaging, and α is a spin projection. The key property of $\hat{\rho}$ in the ODLRO case is the nonzero factorization of the matrix for $|\mathbf{r} - \mathbf{r}_1| \rightarrow \infty$ while $|\mathbf{r}_1' - \mathbf{r}_1|$ and $|\mathbf{r}' - \mathbf{r}|$ remain finite. Then

$$\hat{\rho} \rightarrow \langle \Psi_{\alpha'}^+(r_1') \Psi_{\alpha}^+(r_1) \rangle \langle \Psi_{\alpha}(r) \Psi_{\alpha'}(r') \rangle, \quad (2)$$

i.e., the ODLRO is described by the Gor'kov's order parameter (OP) [3]. For the normal state, $\hat{\rho} \rightarrow 0$ in the same limit.

The possibility of the normal state reconstruction at low temperatures, T , by the boson-mediator induced electron-electron attraction in superconductors [3] inspired the appearance of the mathematically and physically related model called «the excitonic insulator» [7]. In the original BCS model for the isotropic s -pairing the Fermi liquid instability is ensured by the congruence of the Fermi surfaces (FS's) for both spin projections. At the same time, the excitonic instability of the isotropic semimetal is due to the electron-hole (Coulomb) attraction provided both FS pockets are congruent (nested). A similar phenomenon can occur also in narrow-band-gap semiconductors when the exciton binding energy exceeds the gap value [7].

In the excitonic insulator state the two-particle density matrix is factorized in a manner quite different from that of Eq. (2):

$$\hat{\rho} \rightarrow \langle \Psi_{\alpha'}^+(r_1') \Psi_{\alpha}(r) \rangle \langle \Psi_{\alpha}^+(r_1) \Psi_{\alpha'}(r') \rangle, \quad (3)$$

where $|\mathbf{r}_1' - \mathbf{r}_1| \rightarrow \infty$, with $|\mathbf{r}_1' - \mathbf{r}|$ and $|\mathbf{r}' - \mathbf{r}_1|$ being finite. The averages on the right-hand side of Eq. (3) describe the dielectric OP, which will be specified later in the review. One sees that they correspond to the «normal» Green's functions (GF's) \mathcal{G} in the usual notation, whereas the averages in Eq. (2) represent the «anomalous» Gor'kov's GF's \mathcal{F} [3] caused by the Cooper pairing. The long-range order contained in Eq. (3) is called diagonal (DLRO) [7,8]. The classification of ODLRO and DLRO given here is expressed in the electronic representation of the operators rather than in the hole one, for which these notions should be interchanged [8]. However, the difference between two kinds of the long-range order is intrinsic and deep, leading to their distinct coherence properties.

The excitonic insulator state covers four possible different classes of the electronic orderings [7]: CDW's, the spin-density waves (SDW's) characterized below, orbital antiferromagnetism, and spin currents. The last two states have not yet been observed to our knowledge and will be discussed in the following Sections only in brief.

The low- T excitonic rearrangement of the parent electronic phase may be accompanied by a crystal lattice transformation [7,8] due to the electron-phonon coupling, which always exists. Therefore, the Peierls and excitonic insulator models are, in actual fact, quite similar. The main difference is the one-band origin of the instability in the former, while

the latter is essentially a two- or multiple-band entity.

The SDW collective ground state can not only come from the electron-hole pairing but also can be induced by the finite wave-vector singularities of the magnetic susceptibility, whatever the magnitude of the underlying Coulomb electron-electron repulsion [9,10]. SDW's are marked by a periodic spin-density modulation. It can be either commensurate or incommensurate with the background crystal lattice. SDW's with the inherent wave vector \mathbf{Q} , where $|\mathbf{Q}|$ is related to the Fermi momentum k_F (the Planck's constant $\hbar = 1$), were first suggested by Overhauser [11] for isotropic metals. Later the SDW stabilization by band-structure effects, in particular, by nesting FS sections, was shown. SDW's are not so widely abundant as CDW's, their most popular host being Cr and its alloys [10].

In view of the similarities and differences between the DLRO and ODLRO ground states, it seems quite natural that both theorists and experimentalists extensively investigated the coexistence between superconductivity, on the one hand, and CDW's [8,12–19] or SDW's [8,12,15–17,20–22], on the other. The goal of our review is just to cover the main achievements that have been obtained in the study of this issue. It should be stressed that from the theoretical point of view the problem of the coexistence between superconductivity and DW's (hereafter we use the notation DW for the common case of CDW or SDW) in quasi-1D metals is very involved and even in its simplest setup (the so-called *g*-ology) is far from being solved [12,23,24]. On no account can the mean-field treatment, which is our actual method, be fully adequate in this situation. Nevertheless, experiment clearly demonstrates that in real three-dimensional (3D) though anisotropic materials the superconducting and dielectric pairings do coexist in a robust manner, so that the sophisticated peculiarities introduced by the theory of 1D objects remain of academic interest for them. The only, but very important, exception is the organic family (TMTSF)₂X and its relatives [23–25]. Thus, the predictions of the mean-field theory for these very materials should be regarded with a certain caution.

At the same time, for the overwhelming majority of superconductors, suspected or shown to undergo a dielectric transition of the spin-singlet (CDW) or spin-triplet (SDW) type, the main question is not about the coexistence of Cooper and electron-hole pairings (it can be relatively easily proved experimentally), but whether the dielectrization of the FS

is favorable to or destructive of superconductivity. We adopt the latter scenario, being aware of the absence of superconductivity in fully dielectrized substances. Partial dielectrization (gapping) has also been demonstrated to have a detrimental effect on superconductivity [13,23,26,27]. There is also an opposite point of view [28,29], which assumes enhancement of the superconducting critical temperature T_c by the singular electron density of states (DOS) near the dielectric gap edge. This conjecture is based on the model of the doped excitonic insulator with complete dielectrization [8] and has not been verified yet. On the contrary, the model of the partial dielectrization [15–18,20,22], as described below, explains many characteristic features of different classes of superconductors and is consistent with the principal tendency inherent to those substances. Namely, in the struggle for the FS, superconductivity is most often found to be the weakest competitor. Therefore, the most direct way to enhance T_c is to avoid the dielectrization of the DW type [14]. It is, however, necessary to mention the possibility of stimulation of *d*-wave or even *p*-wave superconductivity by DW-induced electron spectrum reconstruction [30].

Irrespective of the utilitarian goals, the physics of DW superconductors is very rich and attractive. In one review it is impossible to consider all sides of the problem or cover all substances which have been claimed to belong to the class of objects concerned. Nevertheless, we shall try at least to mention every type of such superconductors and their characteristics. Special attention is given to oxides, including high- T_c ones. To the authors' knowledge, this aspect of high- T_c superconductivity has not been examined in detail earlier. The theoretical interpretation of the data will be made mainly on the basis of our results, although a large number of the related sources is also involved. We shall not consider alternative scenarios of superconductivity for the low- or high- T_c superconductors treated here, because many of the corresponding comprehensive reviews can be easily found (see, e.g., Refs. 31–36). In those places when it is necessary to indicate the relationships between our approach and other treatments, we often cite reviews rather than original papers because otherwise the list of references would become too lengthy.

Tunnel spectroscopy (TS), point-contact spectroscopy (PCS), and Josephson-effect data for DW superconductors are analyzed in considerable detail because of their great importance in revealing the most salient features of the investigated materials.

The outline of the review is as follows. In Sec. 1 the background experimental data are discussed. High- T_c oxides are considered separately in Sec. 2. A theoretical formulation is given in Sec. 3. The next Sections include theoretical results concerning the specific properties of DW superconductors and discussions of the relevant experimental data. Sections 4 and 5 are devoted to the thermodynamic and electrodynamic properties of DW superconductors. Josephson and quasiparticle currents in junctions involving DW superconductors are studied in Sec. 6. The general conclusions are given at the end of the review.

1. Experimentally observed partially dielectrized superconductors

1.1. CDW superconductors

The most direct way to visualize CDW's in semiconducting and metallic substances is to obtain contrast scanning tunnel microscopy (STM) real-space pictures of their surfaces. Such pictures have been obtained, e.g., for the layered dichalcogenides $1T$ -TaS_{2-x}Se_x [37] and $2H$ -NbSe₂ [38], quasi- $1D$ NbTe₄ [39], and NbSe₃ [40], as well as for the high- T_c oxide YBa₂Cu₃O_{7-x} (YBCO) [41]. At the same time, the application of the spectroscopic STM-based technique enables one to determine the respective dielectric energy gaps. They have been unambiguously found by this method and in related tunnel and point-contact measurements for a number of CDW superconductors: NbSe₃ [40,42–44], $2H$ -NbSe₂ [38,45], $2H$ -TaSe₂ and $2H$ -TaS₂ [45]. In the purple bronze Li_{0.9}Mo₆O₁₇, which reveals a resistivity rise below 25 K and superconductivity below $T_c \approx 1.7$ K [46], the CDW-driven gap was not identified, although the superconducting gap of the conventional BCS type is clearly seen in the tunnel spectra of (Li_{0.65}Na_{0.35})_{0.9}Mo₆O₁₇, with the same T_c as the parent compound [47].

Since CDW's are usually interrelated with crystal lattice distortions [7,8,26,35,46], the detection of the latter often serves as an indicator of the former. Such displacements, incommensurate or commensurate with the background lattice, were disclosed by an x-ray diffraction technique (as momentum-space extra or modified spots) for the perovskites Ba_{1-x}K_xBiO₃ (BKB) [48], which remain candidates for being CDW superconductors, although their high $T_c \approx 30$ K with respect to $T_c \leq 13$ K of their partially dielectrized superconducting relatives BaPb_{1-x}Bi_xO₃ (BPB) [14] may imply total CDW suppression [49]. X-ray diffraction was also helpful for investigating CDW's in the

layered superconductors $2H$ -TaSe₂, $4Hb$ -TaSe₂, $2H$ -TaS₂, $2Hb$ -TaS₂, and $2H$ -NbSe₂ [27,50].

Electron diffraction scattering by the same compounds displayed even more clear-cut CDW patterns [27]. The same method uncovered in BPB a cubic-tetragonal structural instability for $0 \leq x \leq 0.8$ and a tetragonal-monoclinic one for nonsuperconducting compositions, but no incommensurate CDW's [51]. On the other hand, according to the electron diffraction experiments, in Ba_{1-x}A_xBiO₃ (A = K, Rb) the diffuse scattering, corresponding to structural fluctuations of the R_{25} tilt mode of the oxygen octahedra, shows up in the cubic phase near $x = 0.4$ with the highest superconducting T_c [52]. Electron diffraction on K_xWO₃ revealed incommensurate superstructure for $0.24 < x < 0.26$ [53], where T_c has a shallow minimum [54].

Neutron diffraction measurements have revealed structural transitions as well as phonon softening in the oxides Rb_xWO₃ [55], whereas the x-ray diffraction method was unable to discover these anomalies well seen in resistive measurements [56].

Although direct observations of the CDW's are always highly desirable, the lack of them does not ensure the absence of CDW's in the investigated substance. As an example, one should mention the discovery of a weak low- T (≈ 38 K) structural CDW transition in TTF-TCNQ by measurements of the resistivity derivative dp/dT [57]. This result was only subsequently confirmed by the x-ray [58] and neutron [59] scattering. Thus, the existence of CDW's and the concomitant lattice distortion can be established by quite a number of methods. For superconducting layered chalcogenides CDW's manifested themselves in resistivity [26,27] and angle-resolved photoemission spectra (ARPES) [60]. NbSe₃ is a normal structurally unstable metal under ambient pressure P with two successive dielectric phase transitions and becomes superconducting, but still partially dielectrized [44] for $P \geq 0.5$ kbar [61]. Here CDW's were revealed by measurements of the resistivity and heat capacity C_P [5].

In BPB, the partial dielectrization and/or CDW's have been observed both for non-superconducting and superconducting compositions in measurements of ρ and C_P [14], optical reflection spectra [62], and thermopower (TP) [63] (here the coexistence between delocalized and localized electrons made itself evident), and x-ray absorption (EXAFS) [64], where the inequivalence between different Bi ions is readily seen from pair-distribution functions.

Definite evidence for CDW formation in nonsuperconducting and superconducting BKB solid solutions has been obtained in the optical reflection spectra [65] and EXAFS measurements [64]. Moreover, positron angular correlations in BKB disclosed large nesting FS sections [66], which are mandatory for CDW emergence.

Optical reflectance and transmittance investigations of semiconducting BPB compositions with $x = 1, 0.8,$ and 0.6 have elucidated the band-crossing character of the metal–insulator transition there with the respective indirect dielectric gaps $0.84, 0.32,$ and 0.14 eV [67]. The nesting origin of the gap for the limiting oxide BaBiO_3 is confirmed by the band structure calculations [68], according to which the FS nesting is not perfect (see Sec. 3), but the dielectrization is still possible because the BiO_6 octahedron tilting distortions make the FS more unstable against nesting-driven breathing distortions. Similar calculations for BKB with $x = 0.5$ demonstrate the vanishing of both instabilities [68].

Metal–insulator transitions for superconducting hexagonal tungsten bronzes Rb_xWO_3 and K_xWO_3 are observed in resistive, Hall, and TP measurements [54,56]. It is remarkable that the x -dependence of the critical structural transition temperature, T_d , anticorrelates with $T_c(x)$ in Rb_xWO_3 [56] and, to a lesser extent, in K_xWO_3 [54]. On the other hand, such anomalies are absent in superconducting Cs_xWO_3 , where $T_c(x)$ is monotonic [69]. For the sodium bronze Na_xWO_3 superconductivity exists in the tetragonal I modification, and T_c is enhanced near the phase boundary with the nonsuperconducting tetragonal II structure [70]. It may turn out that the recent observation (both by ρ and magnetic susceptibility, χ , measurements) of $T_c \approx 91$ K in the surface region of single crystals $\text{Na}_{0.05}\text{WO}_3$ [71] is due to the realization of an optimal crystal lattice structure without reconstruction detrimental to superconductivity. In this connection one should bear in mind that the oxide Na_xWO_3 is a mixture of two phases, at least for $x \geq 0.28$ [72].

The two-dimensional (2D) $\text{PW}_{14}\text{O}_{50}$ bronze is an example of another low- T_c oxide with a CDW background [73]. Here $T_c \approx 0.3$ K after the almost complete FS exhaustion by two Peierls gaps below $T_{d1} \approx 188$ K and $T_{d2} \approx 60$ K.

The onsets and developments of CDW instabilities in layered dichalcogenides are very well traced by $\rho(T)$ measurements [26]. The characteristic pressure dependences of T_c and T_d are shown in Fig. 1 [26]. One can ascertain once more that CDW's suppress superconductivity, so that for suf-

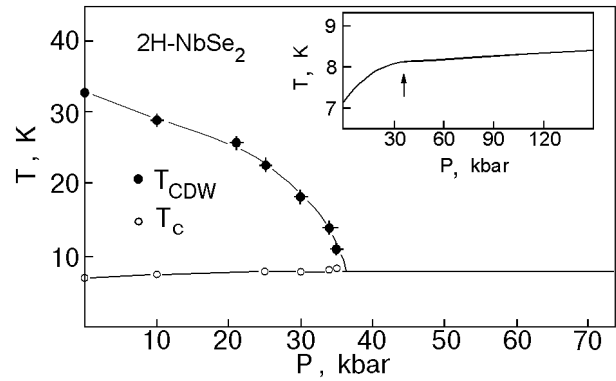


Fig. 1. Phase diagram of the CDW state and of the superconducting state in $2H\text{-NbSe}_2$ from Ref. 26. Inset: pressure dependence of T_c after T. F. Smith, *J. Low Temp. Phys.* 6, 171 (1972).

ficiently high P when $T_d < T_c$, the dependence $T_c(P)$ saturates. For $2H\text{-NbSe}_2$ the ARPES spectra showed the nesting-induced CDW wave vector \mathbf{Q} [60], which agrees with diffraction data [27] and rules out the Rice–Scott scenario of the CDW

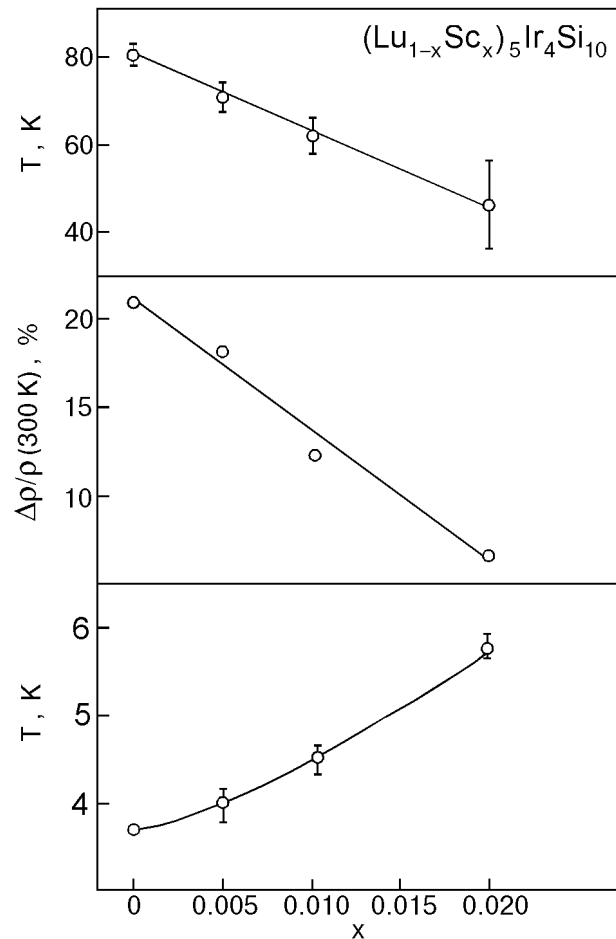


Fig. 2. Alloy concentration dependence of CDW transition temperature T_0 , amplitude of anomaly $\Delta\rho/\rho(300\text{ K})$, and superconducting transition temperature T_c for the pseudoternary system $(\text{Lu}_{1-x}\text{Sc}_x)_5\text{Ir}_4\text{Si}_{10}$ ($x = 0; 0.005; 0.01;$ and 0.02). (from Ref. 77).

appearance due to saddle points of the Van Hove type [35].

Resistive experiments have revealed dielectrization in NbSe₃ as well [5,61]. The addition of Ta was shown to suppress both Peierls instabilities in $\rho(T)$ of this substance [74].

Measurements of ρ and χ under ambient and enhanced pressures have clearly displayed CDW instabilities for Lu₅Ir₄Si₁₀ [75], Lu₅Rh₄Si₁₀ [75,76], R₅Ir₄Si₁₀ (R = Dy, Ho, Er, Tm, Yb, Sc) [75,78], and (Lu_{1-x}Sc_x)₅Ir₄Si₁₀ [77]. The interrelation between T_d , T_c , and the reduced CDW anomaly amplitude $\Delta\rho/\rho(300\text{ K})$ for different compositions of the alloy (Lu_{1-x}Sc_x)₅Ir₄Si₁₀ are exhibited in Fig. 2, taken from Ref. 77.

In the anisotropic compound Tl₂Mo₆Se₆ the CDW instability at $T \approx 80$ K has been observed by Hall, TP, and magnetoresistive (MR) measurements [79].

As to the Chevrel phases, it has been shown in ρ and TP experiments that Eu_{1.2}Mo₆S₈ and its modification Sn_{0.12}Eu_{1.08}Mo₆S₈ are partially-dielectrized (gapped) superconductors [80]. Applied pressure led to the suppression of T_d , a decreasing the degree of dielectric gapping, and the concomitant growth of T_c .

Two well-known structurally unstable superconductor families, namely A15 and C15 compounds (Laves phases), had been investigated in detail before the discovery of high- T_c oxides [13]. Among A15 superconductors is the compound Nb₃Ge, with the highest $T_c \approx 23.2$ K achieved before 1986. Many A15 substances with the highest T_c 's exhibit martensitic transformations from the cubic to the tetragonal structure with T_d slightly (for Nb₃Sn

and V₃Si) or substantially [for Nb₃Al and Nb₃(Al_{0.75}Ge_{0.25})] above T_c . Many lattice properties show strong anomalies at T_d . It was established that the structural transformations had a substantial influence on the superconducting properties. Theoretical interpretations of the electronic and lattice subsystems, electron-phonon interaction, and the interplay between superconductivity and structural instability are based mostly on the assumed quasi-1D features of these compounds [13,81] and will be discussed in the subsequent Sections.

In the C15 compounds HfV₂ ($T_c \approx 9.3$ K) or HfV₂-based pseudobinaries and ZrV₂ ($T_c \approx 8.7$ K) structural anomalies are also present at $T_d \approx 150$ K and ≈ 120 K, respectively [13]. They are detected, e.g., in $\rho(T)$ [13,81] and $\chi(T)$ [13]. Heat capacity measurements [13] have made it possible to observe the corresponding features and even to determine the parameters of the partial-gapping theory.

Competition between CDW's and superconductivity is inherent not only to inorganic substances. For example, in TTF[Ni(dmit)₂]₂, the $\rho(T)$ curves measured at different $P < 14$ kbar demonstrate that at intermediate $P \geq 5.75$ kbar an activated regime above $T_c \approx 2$ K precedes the superconductivity [82]. The suppression of superconductivity by CDW's is also seen in the β_L -phase of quasi-2D (ET)₂I₃ with $T_c \approx 1.2$ K and $T_d \approx 150$ K [25]. At the same time, $T_c \approx 8.1$ K for β -(ET)₂I₃, which shows no traces of CDW's, and superconductivity disappears for α -(ET)₂I₃, which undergoes a metal-insulator transition at 135 K [83].

Key quantities measured for CDW superconductors can be found in Table 1.

Table 1

CDW superconductors

Compound	Reference	P , kbar	T_c , K	Δ , meV	T_d , K	$ \Sigma $, meV	ν	Methods*
NbSe ₃	[61]	8	2.5	—	53	—	—	ρ
	[40]	ambient	—	—	—	80	—	STM
	[44]	— " —	—	—	59	9	—	TS
	[43]	— " —	—	—	59	35	—	STM
Fe _{0.01} NbSe ₃	[43]	— " —	—	—	59	25	—	— " —
Co _{0.03} NbSe ₃	[43]	— " —	—	—	59	48	—	— " —
Gd _{0.01} NbSe ₃	[43]	— " —	—	—	53	0	—	— " —
2H-TaSe ₂	[26]	— " —	0.15	—	120	—	—	ρ
	[45]	— " —	—	—	—	80	—	STM
4Hb-TaSe ₂	[84]	ambient	1.1	—	600	—	—	ρ

Compound	Reference	P , kbar	T_c , K	Δ , meV	T_d , K	$ \Sigma $, meV	ν	Methods*
2H-TaS ₂	[26]	—	0.65	—	77	—	—	—
	[45]	—	—	—	—	50	—	STM
2Hb-TaS ₂	[26]	—	2.5	—	22	—	—	ρ
4Hb-TaS ₂	[84]	—	1.1	—	22	—	—	—
2H-NbSe ₂	[26]	—	7.2	—	33.5	—	—	—
	[45]	—	—	—	—	34	—	STM
Eu _{1.2} Mo ₆ S ₈	[80]	—	0	—	110	—	0.25	ρ , TP
	—	3.2	1.1	—	—	—	0.72	—
	—	7.07	4	—	82	—	1.86	—
	—	9.01	6.4	—	—	—	3.55	—
	—	11.06	8.5	—	66	—	6.7	—
	—	13.2	9.8	—	—	—	∞	—
Sn _{0.12} Eu _{1.08} Mo ₆ S ₈	[80]	ambient	—	—	120	—	0	—
	—	6	1.5	—	100	—	1.22	—
	—	8	3.2	—	78	—	1.86	—
	—	10	7.5	—	—	—	9	—
	—	12	10.1	—	60	—	19	—
Tl ₂ Mo ₆ Se ₆	[79]	ambient	6.5	—	80	—	—	ρ , R_H , TP
ZrV ₂	[13]	—	8.7	—	120	—	—	ρ , χ
	—	—	—	—	—	7.2	0.7	C_p
HfV ₂	[13]	—	8.8	—	150	—	—	ρ , χ
	—	—	—	—	—	8.5	1.1	C_p
Hf _{0.84} Nb _{0.16} V ₂	[81]	—	9.3	—	120	—	—	ρ
	[81]	—	10.7	—	87	—	—	—
Hf _{0.8} Ti _{0.2} V ₂	[81]	—	8.8	—	128	—	—	—
V ₃ Si	[13]	—	17	—	21	—	—	various
Nb ₃ Sn	[13]	—	18	—	43	—	—	—
	[85]	—	—	2.35	—	—	—	TS
	—	—	—	1.12	—	—	—	—
	—	—	—	0.75	—	—	—	—
	—	—	—	0.18	—	—	—	—
	[86]	—	—	2.8	—	—	—	—
	[87]	—	—	2.5	—	—	—	—
Nb ₃ Al	[88]	—	18	—	80	—	—	various
Nb ₃ Al _{0.75} Ge _{0.25}	[13]	—	20	—	24	—	—	—
	[88]	—	18.5	—	105	—	—	—
Nb _{3.08} Al _{0.7} Ge _{0.3}	[88]	—	17.4	—	130	—	—	—
Lu ₅ Ir ₄ Si ₁₀	[75]	—	3.8	—	80	—	—	TE
	[77]	20.5	3.7	—	81	—	—	ρ , χ
(Lu _{0.9} Er _{0.1}) ₅ Ir ₄ Si ₁₀	[77]	ambient	2.8	—	86	—	—	ρ , χ

Compound	Reference	P , kbar	T_c , K	Δ , meV	T_d , K	$ \Sigma $, meV	ν	Methods*
$\text{Lu}_5\text{Rh}_4\text{Si}_{10}$	[77]	23.1	2.74	—	82	—	—	ρ , χ
	[75]	ambient	3.3	—	140	—	—	TE
	[76]	—"	3.4	—	155	—	—	ρ , χ
$\text{P}_4\text{W}_{14}\text{O}_{50}$	[73]	—"	0.3	—	60	—	—	ρ , χ , MR
	—"	—"	0.3	—	185	—	—	—"
$\text{Li}_{0.9}\text{Mo}_6\text{O}_{17}$	[89]	—"	1.7	—	25	—	—	ρ
	[47]	—"	1.5	0.225	—	—	—	TS
$\text{Rb}_{0.25}\text{WO}_3$	[56]	—"	5–7	—	230	—	—	ρ , R_H , TP
$\text{Rb}_{0.24}\text{WO}_3$	[55]	—"	—	—	270	—	—	NS
$\text{Rb}_{0.22}\text{WO}_3$	[55]	—"	—	—	200	—	—	—"
$\text{K}_{0.32}\text{WO}_3$	[54]	—"	2	—	80	—	—	ρ , R_H , TP
$\text{K}_{0.24}\text{WO}_3$	—"	—"	0	—	400	—	—	—"
$\text{K}_{0.2}\text{WO}_3$	—"	—"	1.5	—	280	—	—	—"
$\text{K}_{0.18}\text{WO}_3$	—"	—"	2.5	—	260	—	—	—"
$\text{BaPb}_{0.8}\text{Bi}_{0.2}\text{O}_3$	[90]	—"	11	—	—	4	0.9	C_p
	[91]	—"	11	—	—	4	—	ρ
	[92]	—"	11	—	—	610	—	ORS
	[93]	—"	—	1.15	—	—	—	PCS
	[94]	—"	—	1.25	—	—	—	ORS
$\text{BaPb}_{0.75}\text{Bi}_{0.25}\text{O}_3$	[95]	—"	—	0.77	—	—	—	TS
	[96]	—"	—	1.3	—	—	—	OTS
$\text{BaPb}_{0.73}\text{Bi}_{0.27}\text{O}_3$	[97]	—"	—	1.71	—	—	—	TS
$\text{BaPb}_{0.7}\text{Bi}_{0.3}\text{O}_3$	[98]	—"	—	0.95	—	—	—	—"
	[95]	—"	—	1.5	—	—	—	—"

* N o t a t i o n: ρ stands for resistance, TP for thermopower, R_H for Hall effect, χ for magnetic susceptibility, C_p for specific heat, TE for thermal expansion, MR for magnetoresistance measurements, STM for scanning tunnel microscopy, NS for neutron scattering, and TS for tunnel, ORS for optical reflection, PCS for point-contact, and OTS for optical transmission spectroscopies

1.2. SDW superconductors

The state with coexisting superconductivity and SDW's is observed in the quasi-1D organic substance (TMTSF)₂ClO₄ at ambient pressure [23,25]. Specifically, physical properties of the low- T phase depend on the cooling velocity for $T \leq 22$ K, which was shown in resistive [99], nuclear magnetic resonance (NMR) [100], electron paramagnetic resonance (EPR) [99], and specific heat [101,102] measurements. Rapid cooling (10–30 K/min) leads to the quenched Q -phase with $T_c \approx 0.9$ K, a negative temperature coefficient of resistance (TCR), and SDW's for T less than the Neel temperature $T_N \approx 3.7$ K. A fall in the cooling rate to 0.1 K/min results in the relaxed R -phase with $T_c \approx 1.2$ K, positive TCR, and SDW's existing at $T < 6$ K

[103]. The SDW emergence in the R -phase was verified by the broadening of the NMR line for ⁷⁷Se with cooling [100] and the existence of a $C_p(T)$ singularity at $T \approx 1.4$ K in a magnetic field $H \approx 63$ kOe [101,102].

On the other hand, recent polarized optical reflectance studies of (TMTSF)₂ClO₄ show a broad band, with a gap developed below a frequency of 170 cm⁻¹ [104] and corresponding to collective charge transport [5] by a sliding CDW rather than a SDW. Other reflectance measurements in (TMTSF)₂ClO₄ [103] allowed the authors to extract the gap feature with energy in the range 3–4.3 meV, associated with the SDW gap and substantially exceeding the corresponding BCS weak-coupling value.

It is necessary to emphasize that measurements of the thermal conductivity κ in the substance concerned demonstrate the conventional *s*-like character of the superconducting OP [105]. This fact is at variance with the inclusion [24] of (TMTSF)₂ClO₄ in a large list of superconductors with unconventional pairing. At the same time, this group showed [106] that the electronic contribution to κ is linear in T for the quasi-2D organic superconductor κ -(ET)₂Cu(NCS)₂, so that unconventional superconductivity is really possible there [24]. It also seems quite plausible that this relatively high- T_c (≈ 10.4 K) superconductor is partially gapped well above T_c [107]. Actually, $\rho(T)$ has a broad peak at 85–100 K, with ρ_{peak} 3–6 times as high as $\rho(300$ K). Further decrease of T discloses a metallic trend of ρ and a superconducting transition. See Sec. 5 for subsequent speculations on this matter.

On the basis of the currently available data it is impossible to prove or reject the possibility of SDW persistence in the superconducting state of

(TMTSF)₂X (X = PF₆, AsF₆) existing under external pressure. However, clear SDW-type dielectric-pairing correlations below $T_N \approx 15$ K were revealed in the optical reflectance spectra [108].

The interplay of SDW's and superconductivity has been thoroughly investigated in heavy-fermion compounds [109]. In particular, the magnetic state in URu₂Si₂ is really of the collective SDW type, rather than local moment antiferromagnetism, observed in a number of Chevrel phases and ternary rhodium borides [110], insofar as the same «heavy fermions» are responsible for both collective phenomena. Therefore, the electron subsystem of URu₂Si₂ can be considered below $T_N \approx 17.5$ K (see Table 2) as a partially gapped Fermi liquid [18,22] with appropriate parameters determined by $C_p(T)$ [112–114,116], thermal expansion in an external magnetic field [116], and spin-lattice relaxation [126]. The partial dielectrization concept is supported here by the correlation between the T_c rise and T_N decrease with uniaxial stress [139]. It is

Table 2

Physical parameters of SDW superconductors at ambient pressure

Compound	source	T_c , K	Δ , meV	T_N , K	$ \Sigma $, meV	ν	Methods*
U ₆ Co	[111]	2.5	—	90–150	—	—	ρ
U ₆ Fe	[111]	3.9	—	90–150	—	—	—
URu ₂ Si ₂	[112]	1.3	—	17.5	9.9	0.4	C_p , χ , H_{c2}
	[113]	1.3	—	17.5	11.1	1.5	C_p , ρ , H_{c2}
	[114]	1.2	—	17.5	2.3	—	C_p
	[115]	1.37	—	17.7	5.9	—	TS, PCS
	[116]	—	—	17.5	9.9	—	C_p , TE
	[117]	1.25	—	—	—	—	C_p
	[118]	1.3	0.3	—	—	—	PCS
	[119]	—	—	17.5	10	—	—
	[120]	—	—	—	9.5	—	TS
	[121]	—	0.2	—	—	—	PCS
	[122]	—	0.35	—	—	—	—
	[123]	—	0.17	—	—	—	—
	[124]	—	0.25	—	—	—	—
				(<i>a</i> -axis)			
		—	0.7	—	—	—	—
			(<i>c</i> -axis)				
[125]	—	—	0.35–0.5	—	—	—	TS
[126]	—	—	—	—	12.9	—	NSLR

Compound	source	T_c , K	Δ , meV	T_N , K	$ \Sigma $, meV	ν	Methods*
LaRh ₂ Si ₂	[127]	3.8	—	7	—	—	C_p , ρ , χ
YRh ₂ Si ₂	[127]	3.1	—	5	—	—	— " —
UNi ₂ Al ₃	[128]	1	—	4.6	—	—	— " —
UPd ₂ Al ₃	[120]	1.2	—	4.8	10	—	TS
	[129]	1.9	—	14.3	—	—	C_p , ρ
	[129]	1.9	—	13.8	—	—	χ
	[120]	—	—	—	13	—	TS
	[130]	1.35	0.18	—	—	—	— " —
	[131]	—	—	—	4.5	—	PCS
	[132]	3	—	160	—	7.3	ρ , χ , NMR
CeRu ₂	[133]	6.2	—	50	—	—	ρ , TP, MR, χ , R_H
	[134]	5.4–6.7	0.95–1.3	40–50	—	—	TS
	[135]	6.2	0.6	—	—	—	PCS
	[136]	10.9	1.3	1.5	—	—	— " —
TmNi ₂ B ₂ C	[136]	10.8	1.7	5.9	—	—	— " —
ErNi ₂ B ₂ C	[136]	8.6	1.0	5.2	—	—	— " —
HoNi ₂ B ₂ C	[136]	6.1	1.0	10.5	—	—	— " —
R-(TMTSF) ₂ ClO ₄	[100]	1.2	—	1.37	—	—	NMR
	[103]	—	—	6	3–4.3	—	ORS
Q-(TMTSF) ₂ ClO ₄	[100]	0.9	—	3.7	—	—	NMR
β -(BEDT-TTF) ₂ I ₃	[137]	1–1.5	—	20	—	—	R_H
	[138]	1.5	—	22	—	—	C_p

* See Table 1 for notation and, additionally, H_{c2} for upper critical magnetic field, NSLR for nuclear spin-lattice relaxation, and NMR for nuclear magnetic resonance measurements

interesting that the magnetic neutron scattering Bragg peak (100) exhibits a cusp near T_c , reflecting the superconducting feedback on the SDW, noticeable notwithstanding $T_N \gg T_c$ [140]. In view of the nonconventional behavior of the superconducting OP in heavy-fermion compounds UBe₁₃ and UPt₃ [141], the symmetry of their counterpart in URu₂Si₂ was under suspicion from the very beginning. And recently it was shown that the presence of a line nodes of the OP seems plausible, because the T dependence of the spin-lattice relaxation rate T_1^{-1} does not demonstrate the Hebel–Slichter coherence peak [36] and is proportional to T^3 down to 0.2 K. One should stress, however, that the interplay with SDW's, strong-coupling effects [31], mesoscopic nonhomogeneities [142], and other complicating factors might lead to the same consequences.

There are two other U-based antiferromagnetic superconductors: UNi₂Al₃ and UPd₂Al₃ [143].

Here the transitions to the magnetic states were revealed by studies of ρ , χ , and C_p for both substances, elastic measurements for UPd₂Al₃ [144], and thermal expansion for UNi₂Al₃ [145]. Local ordered magnetic moments in UPd₂Al₃ and UNi₂Al₃ are (0.12–0.24) μ_B and 0.85 μ_B , respectively, as opposed to (10⁻³–10⁻²) μ_B for URu₂Si₂ [146], thus the SDW nature of the antiferromagnetic state for two former compounds remains open to question. The local-moment picture also results from the $d\rho/dT$ continuity for UPd₂Al₃ [147], whereas $d\rho/dT$ for UNi₂Al₃ manifests a clear-cut singularity [148]. Taking into account the distinctions and likeness [120] between various properties of URu₂Si₂, UNi₂Al₃, and UPd₂Al₃, one can conclude that all three compounds are SDW superconductors but with different degrees of magnetic-moment localization.

As to the superconducting OP symmetry, it should be noted that, similarly to URu₂Si₂, the

dependence $T_1^{-1}(T)$ for UPd_2Al_3 exhibits no Hebel–Slichter peak below T_c and $T_1^{-1} \propto T^3$ for low T [149]. Heat capacity for $T \leq 1$ K also has an unconventional contribution $\propto T^3$ compatible with an octagonal d -wave state [147]. However, the problem is far from being solved.

High-pressure investigation of two more heavy-fermion compounds U_6X ($\text{X} = \text{Fe}, \text{Co}$) uncovered an anomalous form of $T_c(P)$, in particular, a kink of $T_c(P)$ for U_6Fe [111]. The authors suggest that these materials undergo transitions to some kind of DW state and identify the kink with the suppression of T_N (or T_d) to a value below T_c .

The compounds LaRh_2Si_2 and YRh_2Si_2 , according to the measurements of their ρ , χ , and C_p , have been also classified as SDW superconductors [127]. Partial gapping of the SDW type was displayed by the investigations of ρ , χ , and C_p for the related substance $\text{Ce}(\text{Ru}_{1-x}\text{Rh}_x)_2\text{Si}_2$ when $x = 0.15$ [150]. However, superconductivity is absent there. This is regrettable, because the results of Ref. 150 demonstrate that the object concerned can be considered as a toy substance for the theory [22], much like URu_2Si_2 [112,113]. FS nesting and SDW's in $\text{Ce}(\text{Ru}_{1-x}\text{Rh}_x)_2\text{Si}_2$ and $\text{Ce}_{1-x}\text{La}_x\text{Ru}_2\text{Si}_2$ were observed in Ref. 151 by neutron scattering.

The cubic SDW superconducting compound CeRu_2 , with the $C15$ -type structure, was found by making use of MR, Hall, TP, and χ measurements [133].

Recently a large family of quaternary borocarbides showing antiferromagnetic and superconducting properties as well as their interplay for the cases $T_c > T_N$ and $T_c < T_N$ was discovered [136]. Incommensurate magnetic structures (SDW's) with the wave vector ($\approx 0.55; 0; 0$), originating from the FS nesting, were found for $\text{LuNi}_2\text{B}_2\text{C}$ [152], $\text{YNi}_2\text{B}_2\text{C}$ [152], $\text{TbNi}_2\text{B}_2\text{C}$ [153], $\text{ErNi}_2\text{B}_2\text{C}$ [154], $\text{HoNi}_2\text{B}_2\text{C}$ [155], and $\text{GdNi}_2\text{B}_2\text{C}$ [156]. It is natural to make the inference that other members of this family possess the same property.

There is a diversity of results regarding the symmetry of the superconducting OP in borocarbides. Namely, $T_1^{-1}(T)$ for $\text{Y}(\text{Ni}_{1-x}\text{Pt}_x)_2\text{B}_2\text{C}$ with $x = 0$ and 0.4 exhibits a Hebel–Slichter peak and an exponential decrease for $T \ll T_c$ [157], which counts in favor of isotropic superconductivity. On the other hand, the T -linear term in the specific heat of $\text{LuNi}_2\text{B}_2\text{C}$ measured under magnetic fields H in the mixed state shows $H^{1/2}$ behavior [158] rather than the conventional H -linear dependence for the isotropic case. Hence, for this class of superconductors the question of symmetry is still open.

Finally, the alloys $\text{Cr}_{1-x}\text{Re}_x$ [10,132] are important SDW superconducting substances, in which the partial gapping is verified by ρ , χ , and NMR measurements.

2. Implications for high- T_c oxides

Already in Ref. 14, while studying BPB, the conclusion was made that structural instability is the main obstacle to high T_c 's in oxides. The validity of this reasoning was proved by the discovery of 30-K superconductivity in BKB [36]. The same interplay between lattice distortions accompanied by CDW's and Cooper pairing is inherent to cuprates, although the scale of T_c is one order of magnitude larger. However, notwithstanding the efficiency of the acting (and still unknown!) mechanism of superconductivity, the existence of the structural instability prevents even higher T_c 's simply because of the partial FS destruction. This key point of our approach is soundly confirmed by experiment.

Thus, thermal expansion measurements on insulating $\text{La}_2\text{CuO}_{4+\delta}$ and $\text{La}_{2-x}\text{M}_x\text{CuO}_4$ ($\text{M} = \text{Ba}, \text{Sr}$) with nonoptimal doping show two lattice instabilities having $T_{d1} \approx 32$ K, $T_{d2} \approx 36$ K, while the underdoped YBCO with $x = 0.5$ and $T_c = 49$ K has a single instability at $T_d \approx 90$ K [159]. Both T_{d2} and T_d are close to the maximal T_c in the corresponding optimally doped compounds. Anomalies of the lattice properties above T_c in $\text{La}_{2-x}\text{M}_x\text{CuO}_4$ were also observed in ultrasound experiments ($x = 0.14$, $\text{M} = \text{Sr}$) [160] as well as in thermal expansion, $C_p(T)$, and infrared absorption measurements [161]. Such anomalies in the vicinity of T_c were shown to be a rule for $\text{La}_{2-x}\text{Sr}_x\text{CuO}_4$ (LSCO), YBCO, and Bi-Sr-Ca-Cu-O [162] and cannot be explained by the superconducting transition *per se* [163]. Rather they should be linked to the structural soft-mode transition accompanying the former [162]. The analysis of the neutron scattering in LSCO shows that the above- T_c structural instabilities reduce T_c for the optimal-doping composition, so that its maximum for $x = 0.15$ corresponds, actually, to the underdoped regime rather than the optimally doped one [164].

It should be noted that in addition to the doping-independent transitions [159] in $\text{La}_{2-x}\text{Ba}_x\text{CuO}_4$ (LBCO) there are also successive transitions from a high-temperature tetragonal (HTT) to a low-temperature orthorhombic (LTO) and then to a low-temperature tetragonal (LTT) phase [35] with T_c suppressed to zero for $x = 1/8$. At the same time, the LSCO phase diagram does not include the LTT

phase, and the superconducting region is not broken [165]. LSCO doped with Nd does have the LTT phase, and this kind of doping is widely claimed to provoke phase separation with either static or dynamic charged and magnetic stripes. In particular, the stripes of the nanoscale width were detected by EXAFS, ARPES, x-ray, neutron, and Raman scattering also in LSCO, $\text{La}_2\text{CuO}_{4+\delta}$, YBCO, $\text{Y}_{1-y}\text{Ca}_y\text{Ba}_2\text{Cu}_3\text{O}_{7-x}$, and $\text{Bi}_2\text{Sr}_2\text{CaCu}_2\text{O}_{8+\delta}$ (BSCCO) [35]. ^{63}Cu and ^{139}La NMR and nuclear quadrupole resonance (NQR) measurements for LSCO with $x = 0.06$ and $T_c \approx 7$ K show that a cluster spin glass emerges below $T_g \approx 5$ K [166]. The authors of Ref. 166 made a conclusion about the freezing of hole-rich regions related to charged stripes below T_g , thus coexisting with superconductivity. The anomalies of the dependences of κ on the planar hole concentration p at $p = 1/8$ in YBCO and $\text{HgBa}_2\text{Ca}_{m-1}\text{Cu}_m\text{O}_{2m+2+x}$ [167] give indirect evidence that the charged stripes (if any) are pinned, probably by oxygen vacancy clusters.

The phase separation concept was introduced long ago for structurally and magnetically unstable systems and later revived for manganites, nickelates, and cuprates [168]. As a microscopic scenario for high- T_c oxides one can choose, e.g., (i) Van Hove singularity-driven phase separation with the density of states (DOS) peak of the optimally doped phase electron spectrum split by the Jahn-Teller effect [35], (ii) droplet formation due to the kinetic energy increase of the extrinsic current carriers at the dielectric gap edge with DOS peaks [169] in the framework of the isotropic model [8], (iii) instability for the wave vector $\mathbf{q} = 0$ in the infinite- U Hubbard–Holstein model, where the local charge repulsion inhibits the stabilizing role of the kinetic energy [170]. In the last case, \mathbf{q} becomes finite when the long-range Coulomb interaction is taken into account. The origin of such incommensurate CDW's (ICDW's) has little to do with the nesting-induced CDW's we are talking about. In practice, nevertheless, ICDW's or charged stripes are characterized by widths similar to the CDW periods in the Peierls or excitonic insulator cases and can be easily confused with each other, especially as the local crystallographic structure is random.

Returning to $\text{La}_{2-x}\text{M}_x\text{CuO}_4$ family, it is important to point out that the atomic pair distribution functions in real space, measured by neutron diffraction both for $\text{M} = \text{Ba}$ and Sr , revealed local octahedral tilts surviving even at high T deep into the HTT phase [171]. For LSCO with $x = 0.115$ electron diffraction has disclosed that low- T struc-

tural transition is accompanied by the CDW's of the $(1/2, 1/2, 0)$ type that lead to the suppression of superconductivity [172]. Raman scattering investigations indicated that in the underdoped case there is a pseudogap $E_{ps} \approx 700 \text{ cm}^{-1}$ without any definite onset temperature, which competes with a superconducting gap for the available FS [173], whereas for the overdoped samples the pseudogap is completely absent [174]. On the other hand, EXAFS measurements for LSCO with $x = 0.15$ and $\text{La}_2\text{CuO}_{4.1}$ have demonstrated that CDW's and superconductivity coexist but with a clear-cut onset temperature T_{es} , revealed from the Debye–Waller factor [175]. The T_{es} 's are doping-dependent and coincide with the corresponding anomalies of the transport properties.

In the YBCO, lattice and, in particular, acoustic anomalies were observed just above T_c soon after the discovery of these oxides [176]. NMR data for YBCO and $\text{YBa}_2\text{Cu}_4\text{O}_8$ confirmed the conclusion that the actual gap below T_c is a superposition of superconducting and dielectric contributions [19,177]. The same can be inferred from the optically determined ac conductivity [178]. Absence of the (^{16}O – ^{18}O)-isotope effect in T_c for $\text{YBa}_2\text{Cu}_4\text{O}_8$ [177] cannot be a true argument against the CDW origin of the normal state gap because the latter may be predominantly of a Coulomb (excitonic) nature (see discussion in Introduction and Sec. 3). There also exists direct STM evidence of the occurrence of a CDW in YBCO [41].

In BSCCO, lattice anomalies above T_c have been observed in the same manner as in LSCO and YBCO [162]. It is remarkable that in BSCCO with $T_c = 84$ K the lowest structural transition is at $T_d = 95$ K, while for Bi-Sr-Ca-Cu-Pb-O with $T_c \approx 107$ K the respective anomaly is at $T_d \approx 130$ K [179], much like the T_c vs. T_d scaling in $\text{La}_{2-x}[\text{Sr}(\text{Ba})]_x\text{CuO}_4$, the YBCO compounds discussed above, and electron-doped cuprates [159]. Local atomic displacements in the CuO_4 square plane of BSCCO due to incommensurate structure modulations have been discovered by the EXAFS method [180]. The competition between superconducting and normal state gaps for the FS in BSCCO was detected in Ref. 181 in an analysis of the impurity suppression of T_c . The other possibility, which fits with a number of theoretical approaches, is a smooth evolution between the gaps while crossing T_c (see, e.g., Ref. 182 and the discussion below), but it is refuted by the experimental data [181]. There is also a good reason to believe that a distinct dip at -90 meV in the ARPES

spectra for BSCCO (see, e.g., the review [183]) is due to dielectric pairing correlations.

The analysis of the relevant experimental data would be incomplete if no mention were made of the incommensurate spin fluctuations revealed by inelastic neutron scattering in $\text{La}_2\text{CuO}_{4+\delta}$, LSCO [184], and YBCO [185], which change from commensurate ones on cooling into the neighborhood of T_c . The phenomenon might be connected, for instance, with the stripe phase state [35,168] or reflect an underlying mechanism of d -wave superconductivity based on antiferromagnetic correlations [33]. It is worth noting that the famous resonance peak with the energy ≈ 41 meV observed by the inelastic neutron scattering in the superconducting state of YBCO is often considered as intimately related to the very establishment of superconductivity [164]. Moreover, *elastic* neutron scattering has shown that there is a long-range SDW order of the mean-field type in $\text{La}_2\text{CuO}_{4+\delta}$ appearing simultaneously with the superconducting transition [186]. Thus, a third player is involved in the game between Cooper pairing and CDW's, making the whole picture rich and entangled. According to Ref. 186, it might be the case that the claimed phase separation in $\text{La}_{1.6-x}\text{Nd}_{0.4}\text{Sr}_x\text{CuO}_4$ [35] is actually a real-space coexistence between superconductivity and SDW's.

Recently ARPES measurements in BSCCO have established an extra 1D narrow electronic band with a small Fermi momentum $k'_F \sim 0.2\pi$ in units of a^{-1} , where $a = 3.8$ Å, in the $\Gamma - M_1 = (\pi, 0)$ direction [187]. For this band, charge (CDW) fluctuations with the nesting wave vector $\mathbf{Q}_c = 2\mathbf{k}'_F$ are expected. The authors associate the spin fluctuations of the wave vector $\mathbf{Q}_s \sim (0.2\pi, 0)$, observed for $\text{La}_{1.6-x}\text{Nd}_{0.4}\text{Sr}_x\text{CuO}_4$ and LSCO [184], with charge fluctuations of the wave vector $2\mathbf{Q}_s$ coinciding with the deduced \mathbf{Q}_c . Later [188] they rejected the allegations [189] that the observed asymmetry of the directions $\Gamma - M = (0, \pi)$ and $\Gamma - M_1$ [187] is an artifact of a misalignment between the rotation axis and the normal to the samples.

Let us return now to the very notion of «pseudogap» («spin gap» or «normal-state gap» [190]). The corresponding features appear in many experiments measuring different properties of high- T_c oxides. This term means a DOS reduction above T_c or an additional contribution to the observed reduction below T_c if the superconducting gap is determined and subtracted. A formal analogy exists here with pseudogaps in the range $T_{3D} < T < T_{MF}$ for quasi-1D or quasi-2D substances, observed both

for dielectric (e.g., Peierls) gaps [5,191] or their superconducting counterparts [27,192,193]. T_{MF} denotes the transition temperature in the respective mean-field theory, while T_{3D} is the actual ordering temperature, lowered in reference to T_{MF} by thermal fluctuations of the order parameter [191,192].

Specifically, pseudogaps with edge energies ≤ 0.03 eV have been detected in $\text{La}_{2-x}[\text{Sr}(\text{Ba})]_x\text{CuO}_4$ by NMR [194], Raman scattering [195], and optical reflection [196]. Furthermore, photoemission measurements have shown that in LSCO there is in addition a «high energy» pseudogap structure at 0.1 eV [197].

In YBCO, pseudogaps have been observed in NMR [177,194], Raman [195], optical reflectance [196], neutron scattering [198], time-resolved quasiparticle relaxation and Cooper pair recombination dynamics [199], specific heat [200], and ellipsometric [178] measurements. Bi-based oxides have exhibited pseudogaps in NMR [194], Raman [195], optical [196], ARPES [201], and resistive [202] experiments. Finally, pseudogaps have been found in Hg-based superconductors with the help of NMR investigations [203].

The origin of the pseudogaps in cuprates is far from being clear [190]. There have been a great many explanations, mostly proceeding from reduced dimensionality, preformed pairs, or giant fluctuations above T_c . For a detailed discussion of this subject see Refs. 35,204. On the contrary, it is natural to conceive the pseudogaps or the related phenomena observed before the pseudogap paradigm became popular as being a result of electron-hole (dielectric) correlations leading to a dielectric gap [35,161,205]. In accordance with this basic concept, the latter coexists with its superconducting counterpart below T_c , whereas above T_c it distorts the FS alone. In recent years this latter point of view has received substantial support, and the calculations have been widened to include anisotropy up to an unconventional, e.g., d -like, character of the dielectric order parameter and the fixation of its phase [19,30,193,206,207]. On the other hand, it is difficult to agree with the conclusions (see, e.g., Ref. 190) frequently drawn from the same body of information, that the superconducting gap Δ emerges from the normal state pseudogap and that the symmetry of the latter is undeniably the d -wave one. A partial character of the dielectric gapping, also accepted in the review [190], may mimic pretty well the purported and often highly desired d -wave order parameter spatial pattern [206,208]. This warning concerns both Δ and the dielectric order parameter Σ , so that contrary to what is usually

stated, the actual order parameter symmetry is not yet understood (see relevant speculations in Refs. 34,36,110,142,193,206). However, the theory outlined below, which is based on the s -wave assumption concerning the order parameter, can be easily generalized to the anisotropic case without any significant changes in conclusions. That is why, also bearing in mind applications to definitely s -wave superconductors, we leave the symmetry issue beyond the scope of this review.

It should be noted that the predominantly $d_{x^2-y^2}$ -type superconducting order parameter of cuprates, inferred mostly from phase-sensitive as well as other experiments, is *not* matched one-to-one with the antiferromagnetic spin fluctuation mechanism of pairing [34]. Actually, in a quite general model including both Coulomb and electron-lattice interactions the forward (long-wavelength) electron-phonon scattering was shown to be enhanced near the phase-separation instability, thus leading to momentum decoupling for different FS regions [209]. In turn, this decoupling can result in an anisotropic superconductivity, e.g., a d -wave one, even for phonon-induced Cooper pairing. Non-screened coupling of the charge carriers with long-wave length optical phonons [210] or anisotropic structure of bipolarons [204] in the framework of the approach of Ref. 32 may also ensure a d -like order parameter structure. There exists an interesting scenario involving the combined action of antiferromagnetic correlations and the phonon mechanism of superconductivity [211]. Namely, correlations modify the hole dispersion, producing anomalous flat bands [212]. Then the robust Van Hove peak in the DOS boosts T_c , Cooper pairing being the consequence of the electron-phonon interaction [211]. In the particular case of cuprates, the buckling mode of the oxygen atoms serves as an input quantity of the Holstein model employed [213].

3. Formulation of the theoretical approach

The theoretical picture outlined below covers two main types of the distorted, partially gapped but still metallic low- T states of the parent unstable high- T phase, which are driven by electron-phonon and Coulomb interaction, respectively. The $1D$ Peierls insulator is the archetypical representative of the first type [1,5,191]. It results from periodic displacements with the wave vector \mathbf{Q} ($Q = 2k_F$) appearing in the ion chain. Here k_F is the Fermi momentum of the $1D$ band above T_d . The emerging periodic potential gives rise to a dielectric gap and all of the filled electronic states are pushed down, leading to an energy advantage superior over the

extra elastic energy cost. The phenomenon discussed is possible because FS sections (Fermi planes at a distance of $2k_F$ in the $3D$ representation) are always congruent (nesting). Then the electron gas response to the external static charge is described by the polarization operator (response function) [191,214]

$$\Pi_{1D}(\mathbf{q}, 0) = 2N_{1D}(0) \frac{k_F}{k_{\perp}} \ln \left| \frac{k_{\perp} + 2k_F}{k_{\perp} - 2k_F} \right|, \quad (4)$$

where \mathbf{q} is the momentum transfer, $\mathbf{q}^2 = k_{\parallel}^2 + k_{\perp}^2$, k_{\parallel} and k_{\perp} are the \mathbf{q} components normal and parallel to the FS, and $N_{1D}(0)$ is the background DOS per spin direction for the $1D$ electron gas. It is precisely the logarithmic singularity of $\Pi_{1D}(\mathbf{q}, 0)$ that drives the spontaneous ion chain distortion — Peierls transition.

This singularity comprises a manifestation of the sharp FS edge in the standing electron wave diffraction. Of course, the same phenomenon survives for higher dimensions but in a substantially weaker form, because the nested FS planes spanned by the chosen wave vector are reduced now (again in the $3D$ representation) to two lines for a $2D$ and to a pair of points for a $3D$ degenerate electron gas [46,214].

Hence, in the $2D$ case we have [214]

$$\Pi_{2D}(\mathbf{q}, 0) = N_{2D}(0) \operatorname{Re} \left\{ 1 - \left[1 - \left(\frac{2k_F}{k_{\perp}} \right)^2 \right]^{1/2} \right\}, \quad (5)$$

where $N_{2D}(0)$ is the $2D$ starting electronic DOS per spin direction. Here the root singularity shows up only in the first derivative of $\Pi_{2D}(\mathbf{q}, 0)$. In three dimensions, the polarization operator $\Pi_{3D}(\mathbf{q}, 0)$ has the well-known Lindhard form, and the logarithmic singularity appears only in the derivative $[d\Pi_{3D}(\mathbf{q}, 0)/dq]_{q \rightarrow 2k_F}$, being the origin of the electron-density Friedel oscillations and the Kohn anomaly of the phonon dispersion relations. The nesting-driven transitions, therefore, seem to be peculiar to $1D$ solids.

In reality, all substances in which the Peierls instability takes place are only quasi- $1D$, although strongly anisotropic, ones [23–25,27,46,191,215]. Then the nesting Fermi planes are warped similarly to what is shown in Fig. 3 for the particular case of the $(\text{TMTSF})_2\text{X}$ compounds [216]. One can see that from the results of the band-structure calculations

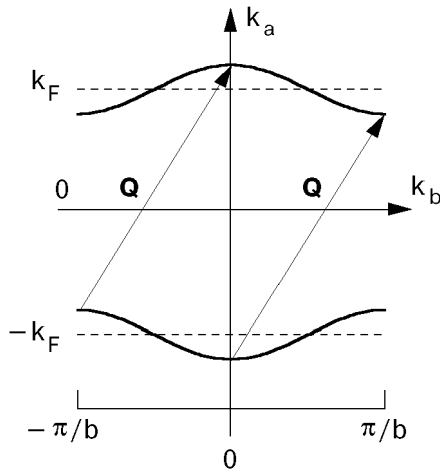


Fig. 3. Two-dimensional view of the open FS for a typical $(\text{TMTSF})_2\text{X}$ compound. The dashed lines represent the planar one-dimensional FS when the interchain hopping rate is zero. The degree of «warping» of the FS is directly related to the electron hopping rate along the b crystal direction (from Ref. 216).

the electronically driven instability is fairly robust and adjusts itself by changing the DW vector \mathbf{Q} , which still spans a finite area of the FS.

Another example, when CDW emergence becomes possible in quasi-2D materials even in the case when the nesting is *imperfect*, was demonstrated by ARPES for SmTe_3 [217]. Here the anomalously strong incommensurate CDW correlations persist up to the melting temperature $T < T_d$, and the measured dielectric gap is 200 meV. But the most interesting observed feature is the inconstancy of the nesting wave vector \mathbf{Q}_{nest} over the nested FS sections. Therefore, although \mathbf{Q}_{nest} no longer coincides with the actual CDW vector \mathbf{Q} , the system still can reduce its energy below T_d !

Finally, one more reason for the instability to survive in the non-1D system is the occurrence of hidden nesting, a concept first applied to the purple bronzes $\text{AMo}_6\text{O}_{17}$ ($A = \text{K}, \text{Na}$), which undergo a CDW phase transition [215]. In these oxides the lowest lying three filled d -block bands make up three 2D non-nested FS's. However, when combined together and with no regard for avoided crossing, the total FS can be decomposed into three sets of nested 1D FS's (see Fig. 4). The wave vector \mathbf{q}_a , which *deviates* from the chain directions, unites two chosen sets of the nested FS sections. Of course, two other nesting wave vectors are possible [46,50,215]. The corresponding superlattice spots in the x-ray patterns as well as ARPES spectra, resistive, Hall effect, and TP anomalies, supporting the hidden-nesting concept, have been observed for $\text{AMo}_6\text{O}_{17}$ [215], Magneli phases

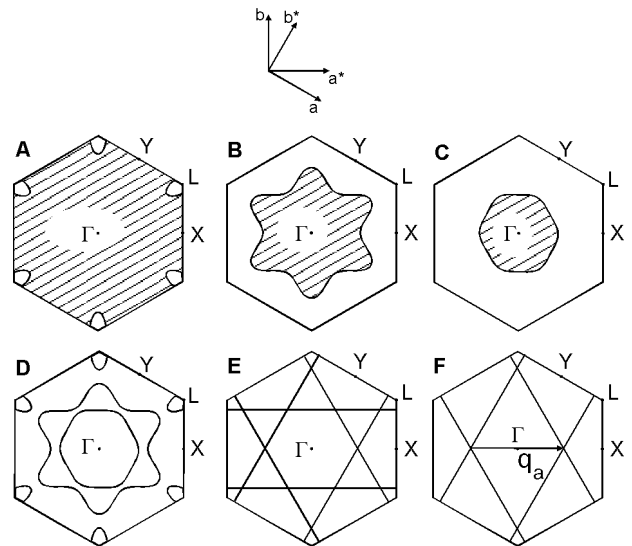


Fig. 4. Hidden nesting in $\text{KMo}_6\text{O}_{17}$. The calculated FS's for the three partially filled d -block bands are shown in A, B, and C, the combined FS's in D, and the hidden 1D surfaces are nested by a common vector \mathbf{q}_a in F (from Ref. 215).

Mo_4O_{11} [50], and monophosphate tungsten bronzes $(\text{PO}_2)_4(\text{WO}_3)_{2m}$ [46,218].

The hidden nesting is inherent also to the layered dichalcogenide family [46,50], which includes CDW superconductors as well (see Table 1). Here, however, the cooperative (band) Jahn–Teller effect can be the driving force for structural modulations [50]. Although the microscopic origin of the Jahn–Teller effect may have nothing to do with the divergence of the polarization operator (4), the loss of the initial symmetry through lattice distortions, appropriate both to the Jahn–Teller low- T state and the Peierls insulator, makes their description quite similar at the mean-field and phenomenological Ginzburg–Landau levels [35,50]. On the other hand, the dynamic band Jahn–Teller effect may be responsible, e.g., for the phase separation in LSCO [35] with mobile walls between LTO and LTT domains.

In 2D systems the Jahn-Teller effect can lead to the degeneracy splitting of two Van Hove singularities [35]. In this connection it is necessary to mention the Van Hove picture of quasi-2D superconductors, especially popular for high- T_c cuprates [35]. The logarithmic singularity of $\Pi_{2D}(\mathbf{Q}_0, 0)$ in the Van Hove scenario stems not from FS nesting but from the logarithmic divergence of the primordial electronic DOS. Here \mathbf{Q}_0 connects two Van Hove saddle points and is CDW vector of a different nature from that for nesting-driven CDW's. Thus it is possible to distinguish between the two scenarios. For cuprates the proper identification is yet

to be done, unlike what has been shown for $2H\text{-NbSe}_2$ [60] (see Sec. 1.1). It should be noted that the Van Hove scenario, extended-saddle-point case included, is often used to explain high T_c 's of oxides [35].

So far, we have envisaged the Peierls instability and concomitant issues, restricting ourselves to the case of noninteracting charge carriers. Of course, the effects of electron-electron interaction should be taken into account properly, which is a very hard job for the case of low-dimensional metals on the verge of instability [12,31,35]. One of the main consequences of the incorporation of many-body effects is a strong screening of the bare Coulomb potentials and the failure of the Fröhlich Hamiltonian to give quantitative predictions for both the normal and superconducting metal properties [12,219]. Nevertheless, these difficulties are not dangerous for our mean-field treatment, in which the existence of the high- T metal – low- T metal phase transition is taken for granted (inferred from experiment!) and we are not trying to calculate the transition temperatures T_d , T_N , or T_c . In any case, the self-consistent theory of elastic waves and electrostatic fields shows that the Peierls transition survives when allowance is made for the long-range charge screening [220].

The SDW state of the low-dimensional metals is treated in substantially the same manner as the CDW Peierls one but with $\Pi_{1D}(\mathbf{q}, 0)$ replaced by the magnetic susceptibility and the electron-phonon interaction replaced by electron-electron repulsion. Usually the approach is simplified, and the latter is described by the simplest possible contact Hubbard Hamiltonian [9]. In the mean-field approximation the subsequent mathematics is formally the same. The only (but essential!) distinction is the spin-triplet structure of the dielectric order parameter matrix.

The other low- T reconstructed state resulting from the primordial semimetallic (or semiconducting) phase is the excitonic insulator phase, the cause of which is the electron-hole (Coulomb) interaction [7,8,12]. The necessary condition for the dielectrization reads

$$\xi_1(\mathbf{p}) = -\xi_2(\mathbf{p} + \mathbf{Q}), \quad (6)$$

where the branch $\xi_{1(2)}$ corresponds to the electron (hole) band, and \mathbf{Q} is the DW vector. This is the nesting (degeneracy) condition we have been talking about, which is automatically fulfilled for a single $1D$ self-congruent electronic band for the Peierls case [1,5,191]. In the general case of an anisotropic metal it is assumed that the condition

(6) is valid for definite FS sections, the rest of the FS remaining intact and being described by the branch $\xi_3(\mathbf{p})$ [18]. All energies $\xi_i(\mathbf{p})$ are reckoned from the Fermi level. Accepting this picture due to Bilbro and McMillan and admitting an arbitrary interplay between electron–phonon and Coulomb interaction [8], we arrive at the general model [18,22] valid for partially gapped «Peierls metals» as well. This model is capable of adequately describing the superconducting properties, as will be readily seen in the subsequent Sections. The excitonic insulator concept presents electron spectrum dielectrization of either the CDW or SDW type [7,8].

Below we consider superconductivity coexisting with DW's, which becomes possible only because of the incomplete character of the FS distortion.

3.1. Generic Hamiltonians of the DW superconductors and the Dyson–Gor'kov equations

The Hamiltonian \mathcal{H}_{el} of such a superconducting electron subsystem

$$\mathcal{H}_{el} = \mathcal{H}_0 + \mathcal{H}_{int} \quad (7)$$

includes the kinetic energy term

$$\mathcal{H}_0 = \sum_{i\mathbf{p}\alpha} \xi_i(\mathbf{p}) a_{i\mathbf{p}\alpha}^+ a_{i\mathbf{p}\alpha}, \quad (8)$$

and the four-fermion interaction processes

$$\begin{aligned} \mathcal{H}_{int} = & \\ = \frac{1}{2} \sum_{\substack{ijklm \\ \alpha\beta}} \sum_{\mathbf{p}\mathbf{p}'\mathbf{q}} V_{ij,lm}(\mathbf{p}, \mathbf{p}', \mathbf{q}) & a_{i,\mathbf{p}+\mathbf{q},\alpha}^+ a_{j,\mathbf{p}'-\mathbf{q},\beta}^+ a_{m\mathbf{p}'\beta} a_{l\mathbf{p}\alpha}. \end{aligned} \quad (9)$$

Here $a_{i\mathbf{p}\alpha}^+$ ($a_{i\mathbf{p}\alpha}$) is the creation (annihilation) operator of the electron in the i th band with quasimomentum \mathbf{p} and spin projection $\alpha = \pm 1/2$;

$$V_{ij,lm}(\mathbf{p}, \mathbf{p}', \mathbf{q}) = V(\mathbf{q}) F_{\mathbf{q}}(i, l | \mathbf{p}) F_{-\mathbf{q}}(j, m | \mathbf{p}')$$

are the matrix elements including electron-phonon and Coulomb contributions and responsible for both superconductivity and dielectrization, and $F_{\mathbf{q}}(i, j | \mathbf{p})$ is a Bloch formfactor determined by the transformational properties of the one-electron wave functions from the i th and j th bands. Moreover, if the antiferromagnetic ordering of the lattice rare-earth ions occurs (as, e.g., in Chevrel phases), the Hamiltonian also incorporates an additional term

$$\mathcal{H}_{AF} = -\mu_B^* \sum_{ij} \sum_{\alpha\beta} \mathbf{H}_{ij}(\mathbf{Q}) \boldsymbol{\sigma}_{\alpha\beta} \sum_{\mathbf{p}} a_{i,\mathbf{p}+\mathbf{Q},\alpha}^+ a_{i\mathbf{p}\beta}, \quad (10)$$

where $\mu_B^* = g^* \mu_B$, μ_B is the Bohr magneton, g^* is the effective g -factor, which is different from 2 due to the crystal field action; $\boldsymbol{\sigma} = \{\sigma_x, \sigma_y, \sigma_z\}$ is a vector composed of the Pauli matrices; and \mathbf{H}_{ij} are matrix elements of the antiferromagnetic molecular field. To consider CDW and SDW superconductors simultaneously, we introduce the notation $\begin{Bmatrix} a \\ b \end{Bmatrix}$, where the upper value corresponds to the CDW case and the lower value corresponds to the SDW one. Then the system Hamiltonian \mathcal{H} reads

$$\mathcal{H} = \mathcal{H}_{el} + \begin{Bmatrix} 0 \\ 1 \end{Bmatrix} \times \mathcal{H}_{AF}. \quad (11)$$

The relevant Dyson–Gor'kov equations for the normal \mathcal{G}_{ij} and anomalous \mathcal{F}_{ij} temperature Green's functions in the general case have the form

$$\begin{aligned} & [i\omega_n - \xi_i(\mathbf{p})] \mathcal{G}_{ij}^{\alpha\beta}(\mathbf{p}, \mathbf{p}'; \omega_n) - \\ & - \sum_{m\gamma\mathbf{k}} \Sigma_{im}^{\alpha\gamma}(\mathbf{p}, \mathbf{k}) \mathcal{G}_{mj}^{\gamma\beta}(\mathbf{k}, \mathbf{p}'; \omega_n) + \\ & + \sum_{m\gamma\mathbf{k}} \Delta_{im}^{\alpha\gamma}(\mathbf{p}, \mathbf{k}) \mathcal{F}_{mj}^{\gamma\beta}(\mathbf{k}, \mathbf{p}'; \omega_n) = \delta_{\mathbf{p}\mathbf{p}'} \delta_{ij} \delta_{\alpha\beta}, \end{aligned} \quad (12)$$

$$\begin{aligned} & [i\omega_n + \xi_i(\mathbf{p})] \mathcal{F}_{ij}^{\alpha\beta}(\mathbf{p}, \mathbf{p}'; \omega_n) + \\ & + \sum_{m\gamma\mathbf{k}} \Sigma_{im}^{+\alpha\gamma}(\mathbf{p}, \mathbf{k}) \mathcal{F}_{mj}^{\gamma\beta}(\mathbf{k}, \mathbf{p}'; \omega_n) - \\ & - \sum_{m\gamma\mathbf{k}} \Delta_{im}^{+\alpha\gamma}(\mathbf{p}, \mathbf{k}) \mathcal{G}_{mj}^{\gamma\beta}(\mathbf{k}, \mathbf{p}'; \omega_n) = 0, \end{aligned} \quad (13)$$

where $\omega_n = (2n+1)\pi T$, $n = 0, \pm 1, \pm 2, \dots$. The normal $\Sigma_{ij}^{\alpha\beta}(\mathbf{p}, \mathbf{k})$ and anomalous $\Delta_{ij}^{\alpha\beta}(\mathbf{p}, \mathbf{k})$ self-energy parts in the weak coupling limit are determined by the well-known self-consistency conditions [3]:

$$\begin{aligned} \Sigma_{ij}^{\alpha\beta}(\mathbf{p}, \mathbf{k}) = & T \sum_{lm\mathbf{q}, \omega_n} \left[V_{im,lj}(\mathbf{p}-\mathbf{q}) \mathcal{G}_{lm}^{\alpha\beta}(\mathbf{q}, \mathbf{q}+\mathbf{k}-\mathbf{p}; \omega_n) - \right. \\ & \left. - \delta_{\alpha\beta} V_{im,jl}(\mathbf{p}-\mathbf{q}) \sum_{\gamma} \mathcal{G}_{lm}^{\gamma\gamma}(\mathbf{q}, \mathbf{q}+\mathbf{k}-\mathbf{p}; \omega_n) \right] + \\ & + \boldsymbol{\sigma}_{\alpha\beta} \mathbf{H}_{ij}(\mathbf{Q}) \times \begin{Bmatrix} 0 \\ 1 \end{Bmatrix}, \end{aligned} \quad (14)$$

$$\Delta_{ij}^{\alpha\beta}(\mathbf{p}, \mathbf{k}) =$$

$$= T \sum_{lm} \sum_{\mathbf{q}, \omega_n} V_{ij,lm}(\mathbf{p}-\mathbf{q}) \mathcal{F}_{lm}^{\alpha\beta}(\mathbf{q}, -\mathbf{q}+\mathbf{k}+\mathbf{p}; \omega_n). \quad (15)$$

For the special case of contact interactions, when the matrix elements $V_{ij,lm}(\mathbf{q})$ no longer depend on \mathbf{q} , it happens that

$$\Sigma_{ij}^{\alpha\beta}(\mathbf{r}, \mathbf{r}') = \Sigma_{ij}^{\alpha\beta}(\mathbf{r}) \delta(\mathbf{r} - \mathbf{r}'), \quad (16)$$

$$\Delta_{ij}^{\alpha\beta}(\mathbf{r}, \mathbf{r}') = \Delta_{ij}^{\alpha\beta}(\mathbf{r}) \delta(\mathbf{r} - \mathbf{r}') \quad (17)$$

in real space, corresponding to

$$\Sigma_{ij}^{\alpha\beta}(\mathbf{p}, \mathbf{k}) = \Sigma_{ij}^{\alpha\beta}(\mathbf{p} - \mathbf{k}), \quad (18)$$

$$\Delta_{ij}^{\alpha\beta}(\mathbf{p}, \mathbf{k}) = \Delta_{ij}^{\alpha\beta}(\mathbf{p} + \mathbf{k}) \quad (19)$$

in momentum space. Hereafter we adopt the strong mixing approximation for states from different FS sections [18]:

$$V_{ii,ii} = V_{ii,jj} = V_{ii,33} \equiv -V < 0 \quad (i, j = 1, 2). \quad (20)$$

The opposite case of the weak mixing reduces in essence to the problem of superconductivity in a Keldysh-Kopaev isotropic semimetal [8], while the intermediate case of arbitrary relationships between various matrix elements is the most realistic but does not involve any new qualitative features in comparison to the strong mixing case.

As a consequence of Eq. (20) one has $\Delta_{ij}^{\alpha\beta}(\mathbf{p}, \mathbf{k}) = \Delta^{\alpha\beta} \delta_{ij}$, and a single superconducting order parameter $\Delta^{\alpha\beta}$ develops on the whole FS. We restrict ourselves to singlet superconductivity [3]:

$$\Delta^{\alpha\beta} = \mathbf{I}^{\alpha\beta} \Delta, \quad (\mathbf{I}^{\alpha\beta})^2 = -\delta_{\alpha\beta}. \quad (21)$$

Due to the gauge invariance of Eqs. (12) and (13), the superconducting order parameter Δ can be taken as positive real. On the other hand, the matrix $\Sigma_{ij}^{\alpha\beta}(\mathbf{p}, \mathbf{k})$ has the only nonzero components $\Sigma_{12}^{\alpha\beta} = \Sigma_{21}^{\alpha\beta} \equiv \Sigma^{\alpha\beta}$ and may be either singlet or triplet:

$$\Sigma^{\alpha\beta} = \Sigma \times \begin{Bmatrix} \delta_{\alpha\beta} \\ (\boldsymbol{\sigma}_z)_{\alpha\beta} \end{Bmatrix}. \quad (22)$$

We shall consider the DW's to be pinned, i.e., we confine ourselves to electric fields (if any) below the threshold values, so that the coherent phenomena [5,221] are not taken into account. Thus, the phase of the dielectric order parameter Σ is fixed

[8,222] (see also the discussion in Sec. 6.4). It is determined as well by the matrix elements of the one-particle interband transitions and the molecular field $\mathbf{H}(\mathbf{Q})$, if any [17]. We shall consider Σ to be real of either sign, since its imaginary part would correspond to the as-yet unobserved states with current-density (singlet $\Sigma^{\alpha\beta}$) or spin-current-density (triplet $\Sigma^{\alpha\beta}$) waves [7,8,59, 169,193,194,222].

4. Theoretical description of thermodynamic properties and comparison with experiment

It is natural that the occurrence of two gaps, superconducting and dielectric, on the FS will change thermodynamic properties of DW superconductors as compared to BCS superconductors or partially dielectrized normal metals. In the absence of impurities and making allowance for only the paramagnetic effect of the external magnetic field, the system becomes spatially homogeneous, and the Dyson–Gor’kov equations are essentially simplified.

4.1. Superconducting and dielectric gaps

When the matrix structure of the OP’s in the spin and the FS section spaces is separated out [15,17,20], their amplitudes, Δ and Σ , become (generally speaking, T -dependent) quantities to be found from a set of two integral equations in a self-consistent manner. As was stressed in the Introduction, the relations between Δ and Σ are antagonistic, and they tend to reduce each other. The external magnetic field \mathbf{H} also contributes to this competition, introducing an additional term

$$\mathcal{H}_{\text{ext}} = -\mu_B^* \sum_{i\rho\alpha\beta} (\sigma_{\alpha\beta} \mathbf{H}) a_{i\rho\alpha}^+ a_{i\rho\beta} \quad (23)$$

to the Hamiltonian of the system \mathcal{H} with appropriate modifications of Eqs. (12) and (13) [15,17]. Assuming constant densities of states on the dielectrized, $N_d(0)$, and non-dielectrized, $N_{nd}(0)$, FS sections, with

$$N(0) = N_d(0) + N_{nd}(0) \quad (24)$$

being the total DOS at the Fermi level, the following equation binding Δ , Σ , T and $h = \mu_B^* H$ can be obtained from Eq. (15) [15,17]:

$$1 = \frac{1}{2} V N_{nd}(0) I(\Delta) + \frac{1}{2} V N_d(0) I_d, \quad (25)$$

where

$$I(\Delta) = \int_0^\Omega \frac{d\xi}{\sqrt{\xi^2 + \Delta^2}} \left(\tanh \frac{h + \sqrt{\xi^2 + \Delta^2}}{2T} - \tanh \frac{h - \sqrt{\xi^2 + \Delta^2}}{2T} \right), \quad (26)$$

Ω is the relevant cutoff frequency of the predominantly electron-phonon interaction V ; and the quantity I_d is equal to $I_d^{CDW} = I(D)$ for the CDW case with

$$D(T) = \sqrt{\Delta^2(T) + \Sigma^2(T)} \quad (27)$$

and to $I_d^{SDW} = (1/2\Delta) [D_+ I(D_+) + D_- I(D_-)]$ for the SDW case with

$$D_\pm(T) = \Delta(T) \pm \Sigma(T). \quad (28)$$

The control parameter [18]

$$v = N_{nd}(0)/N_d(0) \quad (29)$$

characterizes the degree of the FS dielectrization and varies from infinity, which corresponds to the absence of FS dielectrization, to zero in the case of full dielectrization. It can be changed experimentally, e.g., by applying an external pressure to the sample (see, e.g., Ref. 80).

Another equation describing the feedback influence of Δ on Σ can be obtained using Eq. (14). This equation and Eq. (15) comprise a self-consistent set. As a consequence, the explicit $\Sigma(T)$ dependences differ from those appropriate to the normal state. But if T_d or T_N strongly exceed T_c , self-consistency of the calculations is not mandatory, and the explicit dependence $\Sigma(T)$ is not crucial for the investigation of superconducting properties. For example, in the framework of the adopted simplified scheme, we may select $\Sigma = \text{const} = \Sigma_0$ in the whole range $0 < T < T_c$ (in this Section $\Sigma > 0$ without any loss of generality) and insert this value into Eq. (15) to calculate $\Delta(T = 0)$ and T_c in the absence of the magnetic field. The explicit analytical expressions can be found elsewhere [15,17]. Calculations show that for both DW cases the dependences of T_c / Δ_0 on $\sigma_0 \equiv \Sigma_0 / \Delta_0$, where Δ_0 is the magnitude of the superconducting gap when the FS dielectrization is absent ($v \rightarrow \infty$), are monotonically decreasing, becoming very steep for small v ’s.

It is interesting to examine the ratio $\Delta(0)/T_c$ and compare it with a classical BCS value $\pi/\gamma \approx 1.76$, where $\gamma = 1.781\dots$ is the Euler constant. Relevant calculations demonstrate that in the case of CDW superconductors the dielectrization leads to $\Delta(0)/T_c$,

which is always smaller than π/γ . The deviations from this value are substantial for small v . It is known [219] that a strong electron-phonon coupling increases the ratio. In moderate- T_c superconductors these effects may compensate each other. Perhaps that is why the BCS relation between $\Delta(0)$ and T_c is fulfilled well [223] in a BPB with an unstable structure [14], despite the fact that T_c is as high as 10 K there. It seems that, in order to check the theory, it will be necessary to carry out comprehensive measurements of the superconducting energy gaps in a certain class of compounds including superconductors with and without CDW's.

On the other hand, for SDW superconductors the theoretical dependences of $\Delta(0)/T_c$ on σ_0 are more involved, and the ratio concerned may be either larger or smaller than π/γ [15]. This quantity changes drastically when $\sigma_0 \approx 0.7$, which corresponds to $\Sigma_0/T_c \approx 1.5$. This fact can lead, e.g., to a strong dependence of $\Delta(0)/T_c$ on external pressure. A comparison of the obtained results with the experiment for organic Bechgaard superconductors $(\text{TMTSF})_2\text{X}$ is difficult, because various measurements result in different Δ values, and one cannot rule out the emergence of fluctuation-like pseudogaps there [23]. At the same time, in Cr-Re alloys, where $\Delta(0)$ was determined through the nuclear spin-lattice relaxation rate [132], the quantity $\Delta(0)/T_c$ proved to be from 1.4 to 1.6, which speaks in favor of our theory. In URu_2Si_2 , the toy SDW superconductor, this ratio comprises 80% of the BCS value [121], contrary to the speculations [224] that the antiferromagnetic ordering in the anisotropic compound should increase $\Delta(0)/T_c$ over π/γ .

It is easy to calculate the T behavior of $\Delta(T)$ in the vicinity of T_c . The analysis shows that for small enough v 's the superconducting transition in the SDW case becomes first-order [17,225]. The numerical calculations of the dependence $\Delta(T)$ in the whole interval $0 < T < T_c$ show that although the amplitude of Δ strongly depends both on Σ and v values, the forms of the $\Delta(T)/\Delta(0)$ curves plotted as functions of the normalized temperature $\theta = T/T_c$ differ insignificantly from the Mühlischlegel curve [3] for both DW cases [226].

4.2. Heat capacity

It seems natural that the very existence of the dielectric gap affects the T behavior of the specific heat C_s for DW superconductors. Actually, however, the inductive method did not reveal a jump $\Delta C = C_s - C_n$, where C_n is the specific heat of the normal (although dielectrized) phase near the criti-

cal temperature T_c , for the CDW superconducting ceramics BPB with $x = 0.25$ [227]. This result was supported by measurements of the thermal relaxation rate [228]. At the same time, a partial removal of the FS dielectrization in this substance results in the appearance of a jump ΔC measured by adiabatic calorimetry [90]. The anomaly is also seen in sensitive ac calorimetric measurements of BPB single crystals [229]. The experiments on the Laves phases HfV_2 and ZrV_2 [13] demonstrated that the ratio $\Delta C/\gamma_S T_c$ (γ_S is the Sommerfeld constant) is considerably smaller than the relevant BCS value $12/7\zeta(3) \approx 1.43$, where $\zeta(x)$ is the Riemann zeta function. On the other hand, for SDW superconductors the situation is much more complicated. For example, the ratio $\Delta C/\gamma_S T_c$ for the organic salt $(\text{TMTSF})_2\text{ClO}_4$ depends substantially on the cooling rate. All these facts and those discussed below may be explained in the framework of the adopted scheme.

From a comparison of the free energies for superconducting and normal phases [17] it follows that a phase where CDW's and superconductivity coexist is the ground state of the anisotropic metal whatever the value of v . At the same time, the SDW superconducting phase is possible only if $v > \Delta^2(0)/6\Sigma^2$. This condition does not coincide with the criterion of Machida and Matsubara [225], who determined incorrectly the ground-state energies of the competing phases. According to our estimates, the coexistence of SDW's and superconductivity can be achieved only if the development of the dielectric gap is compensated by the appropriate reduction of the reconstructed FS section area.

On the other hand, assuming that for both cases (CDW and SDW) the phase transition to the superconducting state is second-order and carrying out the standard procedure [3] for the region $T \approx T_c$, we find that the main correction to the BCS relationship $\Delta C/C_n = 1.43$ is quadratic in (T_c/Σ) , reduces the specific heat jump at T_c for CDW superconductors, and enhances it for SDW ones [17].

The reduction of the specific heat anomaly at $T = T_c$ in CDW superconductors was actually observed for a BPB solid solution with a distorted perovskite structure [14]. The jump ΔC was absent for superconducting samples with $T_c = 10$ K after prolonged storage, whereas their diamagnetic Meissner properties remained unchanged. The high-temperature annealing led to a restoration of the initial dependence $C(T)$. Such a behavior can be explained by an increase of the area of the dielectrized FS section during aging, perhaps, due to

oxygen diffusion. Measurements for BKB with $x = 0.4$ also show either a total absence of the anomaly for polycrystals [230] or a 60% reduction [231] in comparison with the expected discontinuity [232], calculated on the basis of the BCS theory from the upper critical magnetic field $H_{c2}(T)$ data. Our explanation of the results for BKB with the help of the partial dielectrization model seems much less exotic than the alternative theory describing the superconducting transition in BKB as a fourth-order one in the Ehrenfest sense [233].

An anomalously small $\Delta C/\gamma_S T_c \approx 0.6$ was observed [234] in $\text{Li}_{1.16}\text{Ti}_{1.84}\text{O}_4$ with $T_c^{\text{onset}} \approx 9$ K, dielectrized by a variation of the composition relative to the parent compound LiTi_2O_4 , with $T_c^{\text{onset}} \approx 12.6$ K. Unfortunately, data available for high- T_c oxides, being the most important CDW superconductors, are almost of no help for detecting the peculiarities predicted by the partial-gapping model. In YBCO, e.g., it is claimed [235] that the mean-field picture itself does not exist here, so that instead of the clear-cut jump ΔC a λ -like anomaly takes place, which reflects the Bose–Einstein-condensation rather than Cooper-pairing nature of the superconducting transition. The smearing of the jump is observed for other oxide families as well [236]. The unresolved question about the superconducting OP symmetry also makes the whole problem very involved [237] and at the time it is only possible to state that there is a tendency for the anomaly ΔC to be less than is required by the BCS or, especially, by the strong-coupling theory [219].

On the other hand, the properties of the SDW organic superconductor $(\text{TMTSF})_2\text{ClO}_4$ [99–102] depend on the thermal treatment, especially the cooling rate when $T \leq 22$ K (see Section 1.2). According to Refs. 101,102, the ratio $\Delta C/\gamma_S T_c = 1.67 > 1.43$ in the R -phase. In the Q -phase the reduction of T_c is accompanied by a fall of $\Delta C/\gamma_S T_c$ to 1.10–1.14 [101], which is less than 1.43. The contradiction with our theory is apparent because the FS gapping leads also to a reduction of the ratio $N_{nd}(0)/N(0)$ and hence to a decrease of the Sommerfeld constant $\gamma_S \propto N_{nd}(0)$. At the same time, the latter value of $\Delta C/\gamma_S T_c$ was calculated using $\gamma_S \approx 10.5$ mJ/mol·K² for the R -phase [102]. Thus, in order to compare the theory and the experiment it is necessary to measure γ_S directly in the Q -phase. The quantity $\Delta C/\gamma_S T_c$ also exceeds the value 1.43 in other compounds, e.g., it equals 1.5 in $\beta\text{-(ET)}_2\text{I}_3$ [25], 2.1 in U_6Fe [238] (the controversy CDW vs. SDW not yet resolved), 2 in CeRu_2 [239]. The same is true for different borocar-

bides [240]. It is reduced, however, in URu_2Si_2 [224].

One should note that the major experimental trend in $\Delta C/\gamma_S T_c$ for SDW superconductors is in agreement with the outlined theory and contradicts the opposite tendency predicted in Ref. 224. On the other hand, the scenario of the Van Hove singularity-determined superconductivity, closely related to ours, always leads to $\Delta C/\gamma_S T_c > 1.43$ [241], the excess being larger for s wave order parameter symmetry than for d wave.

4.3. Impurity effects

Soon after the formulation of the BCS theory for pure isotropic metals the theoretical investigation of dirty superconductors began. In particular, it was shown that in the framework of the BCS scheme nonmagnetic impurities do not alter T_c (the Anderson theorem) [3]. At the same time, magnetic impurities inhibit superconductivity due to their non-symmetrical interaction with components of the spin-singlet Cooper pair [242]. The Anderson theorem is invalid if one goes beyond the scope of the BCS scheme, namely, if the translational invariance is absent (the proximity effect) [243], or if the strong coupling is taken into account, when the impurity renormalization of the electron-phonon kernel of the Eliashberg equation is essential [244]. In the latter case T_c increases with the nonmagnetic impurity concentration n . But there is an opposite and stronger effect [245], consisting in the reduction of the phase space available to electron-phonon interaction, since the low-frequency phonons become «ineffective». The combination of these factors leads to degradation of T_c .

Nonmagnetic impurities also change T_c in superconductors with complicated FS's [246]. In particular, it was shown [247], that in compounds with fine electron DOS structure, such as A15, nonmagnetic impurities, e.g., radiation defects, raise or lower T_c due to the smearing of the DOS peaks near the FS.

All of the above-mentioned reasons, except the last, result in a decreasing function $T_c(n)$. At the same time, the opposite behavior was observed when superconductors were irradiated by neutrons or fast ions [248] or were disordered [88]. In high- T_c oxides nonmagnetic impurities were demonstrated to substantially reduce T_c [34,36], which served as a sound argument when treating these objects as unconventional ones [34].

It is shown [20] that the interference between the electron spectrum dielectrization and the impurity scattering can change T_c in DW superconduct-

tors, thus explaining a large body of evidence both for low- and high- T_c compounds. To consider the influence of impurity scattering on the critical temperature T_c in DW superconductors, we added new terms to the Hamiltonian \mathcal{H}_{el} [Eq. (7)], describing electron-impurity interactions [20]. The calculations are straightforward [242], although cumbersome, and give explicit analytical results in the case $|\Sigma| \gg T_c$. Here only the most significant result for nonmagnetic impurities in the above-defined limit is presented. Namely [20]

$$T_c \approx \left(\frac{\pi T_{c0}}{\gamma |\Sigma| \times \left\{ \frac{1}{\bar{e}} \right\}} \right)^{1/\nu} \left(1 + \frac{\pi}{8\nu |\Sigma| \tau_d} \times \left\{ \frac{1}{3} \right\} \right), \quad (30)$$

where τ_d is the impurity relaxation time for quasiparticles from the degenerate FS sections, $T_{c0} \equiv (\gamma/\pi)\Delta_0$, and \bar{e} is the base of natural logarithms. Thus, T_c in DW superconductors is sensitive to nonmagnetic impurities or defects. This effect does *not* reduce to a well-known result for the electron-hole pair breaking by the Coulomb field of impurities [7]. The obtained violation of the Anderson theorem is caused by the fact that the single-particle states composing the Cooper pairs are in reality superpositions of electrons and holes. Hence, the Cooper pair components are not interrelated, as usual, by the time inversion operation.

While comparing these theoretical results with experimental data, one should bear in mind that, e.g., $A15$, $C15$, and the Chevrel phases have involved band structures. Therefore, even a small disorder alters the latter, and hence T_c , drastically. Degradation of T_c due to this kind of electron spectrum distortion has been considered in detail in Ref. 249. But in experiments dealing with the irradiational damage of superconductors with unstable crystal lattices the T_c degradation sometimes changes to enhancement or saturation. This occurs, e.g., in Nb_3Ge and Nb_3Sn irradiated by ^{16}O and ^{32}S ions [247,248]. Moreover, for low- T_c superconductors with the $A15$ structure a significant growth of T_c is observed after the exposure to the particle irradiation: α -particles in the case of Mo_3Ge and ^{32}S ions in the cases of Mo_3Ge and Mo_3Si [13]. Concerning the superconducting Laves phases HfV_2 and ZrV_2 , which possess enhanced radiation stability of T_c , they exhibit an increase of T_c as the degree of atomic order decreases [13]. In layered compounds $2H-TaS_2$ and $2H-TaSe_2$ the irradiation by electrons with energy 2.5 MeV leads to a discernible rise of T_c [250]. As for high- T_c oxides,

their anomalously high sensitivity to atomic substitution seems to be related to the marginal existence of the relevant crystal structures favorable for the very occurrence of superconductivity. In this respect they are very similar, e.g. to $A15$ compounds. The small effect of the T_c growth predicted in Ref. 20 appears to be subdominant here.

5. Theoretical description of electrodynamic properties and comparison with experiment. Upper critical magnetic field

For a number of superconducting materials (in particular, high-field ones) the temperature dependences of the upper critical magnetic field $H_{c2}(T)$ differ substantially from that obtained in the framework of the BCS theory [251]. Their most striking feature is the positive curvature $d^2H_{c2}/dT^2 > 0$, the values of H_{c2} often diverging for low T thus even exceeding the paramagnetic limit [15]. Besides the trivial explanation making allowance for the macrostructural distortion in superconductors with low dimensionality (see, e.g., [252]) many other mechanisms have been proposed. These include, for instance, FS and OP anisotropy [253], the presence of several groups of current carriers [254], compensation of the external magnetic field by localized magnetic moments [255] (the Jaccarino–Peter effect [242]), the size effect in layered or granular systems with Josephson coupling between constituents [256], extremely strong electron-phonon coupling [257], $2D$ conventional [258] or extended [259] Van Hove singularities, the enhancement of the Coulomb pseudopotential in weakly [260] and strongly [261] disordered metals due to the Altshuler-Aronov effect [262], the influence of the magnetic field on the diffusion coefficient in the vicinity of the Anderson transition [263], fluctuation renormalization of the coherence length [263], and a bipolaronic mechanism of superconductivity [32]. The main shortcoming of these scenarios is that in every case they are confined to a definite class of superconducting materials.

At the same time, most superconductors with deviations of $H_{c2}(T)$ from the BCS behavior are DW superconductors. The effect of the electron-spectrum degeneracy on H_{c2} was considered first in a simplified quasi- $1D$ model with a complete FS dielectrization both for CDW [264] and SDW [265] cases. In our view, the main results of these papers are erroneous, since the obtained corrections to the electromagnetic kernel are proportional to Σ/E_F (SDW case) or $(\Sigma/E_F)^2$ (CDW case), where E_F is the Fermi energy. Such corrections cannot be taken into account in principle by a BCS-type

theory. The correct calculations in the same quasi-one dimensional model were carried out later [266] for an SDW superconductor with $T_N < T_c$.

The more realistic model of DW superconductors with partial FS dielectrization and T_d , $T_N > T_c$ has been investigated in a previous paper [16]. At the end points of the temperature interval $0 < T < T_c$ the expressions for $H_{c2}(T)$ read

$$H_{c2}(T \rightarrow 0) \approx \frac{\pi c T_c}{2\gamma e D_{nd}} \left(1 - \frac{\pi^2 A}{4\gamma} \right) \left[1 - \frac{2}{3} \left(\frac{\gamma T}{T_c} \right)^2 \right], \quad (31)$$

$$H_{c2}(T \rightarrow T_c) \approx \frac{4c T_c (1 - T/T_c)}{\pi e D_{nd} (1 + 2A)} \times \left[1 - \frac{1/2 - 28\zeta(3)/\pi^4 - 2A^2}{(1 + 2A)^2} \left(1 - \frac{T}{T_c} \right) \right], \quad (32)$$

$$A = \left\{ \frac{1}{1/3} \right\} \times \frac{T_c D_d}{\pi v \Sigma^2 \tau_d D_{nd}}. \quad (33)$$

Here c is the speed of light; $D_i = v_i^2 \tau_i / 3$ are the diffusion coefficients for electrons from the degenerate ($i = d$) and nondegenerate ($i = nd$) FS sections; v_i are the Fermi velocities; and τ_{nd} is the relaxation time for the nondielectrized FS section.

From Eqs. (31) and (32) it follows that the appearance of the dielectric gap leads to the reduction of the effective electron-diffusion coefficient $D_{\text{eff}} \approx D_{nd}(1 + A)$. Such a renormalization is to a certain extent analogous to the diffusion coefficient reduction in «dirty» superconductors due to the weak Anderson localization [260]. Also we see that for DW superconductors Eqs. (31) and (32) predict large values of $H_{c2}(0)$ and $|dH_{c2}/dT|_{T=T_c}$. Moreover, according to Eq. (32) and provided v is small, a positive curvature of $H_{c2}(T)$ is possible, although not inevitable.

These conclusions agree well with the experimental data for CDW superconductors. In particular, the positive curvature is observed for $A15$ compounds Nb_3Sn and V_3Si . In agreement with Eq. (32), for the tetragonal (partially gapped) phase of Nb_3Sn the slope $|dH_{c2}/dT|_{T=T_c}$ is always larger than in the cubic phase [13]. In this compound a decrease of sample purity, which is accompanied by a suppression of the structural transition, also results in the change of a sign of d^2H_{c2}/dT^2 from positive to negative. At the same time, the observed dependence of d^2H_{c2}/dT^2 on the sample resistivity seems to rule out the interpretation [261] of the

experimental data for Nb_3Sn in the framework of the theory taking into account the influence of strong localization on the Coulomb pseudopotential.

The change in of the curvature sign can be achieved by varying the parameter v . The simplest ways here are to apply an external pressure or to change the composition. The latter was implemented for BPB solid solutions, where $d^2H_{c2}/dT^2 > 0$ was observed both for superconducting ceramics [267] and single crystals [268]. The following fact is of fundamental importance here: positive curvature of the critical field exists only for compounds with $x \geq 0.2$ (i.e., close enough to the metal–semiconductor transition at $x \approx 0.4$), for which numerous experimental data show the appearance of a dielectric gap on the FS (see Section 1.1). The composition dependence rules out another explanation [269] of the relation $d^2H_{c2}/dT^2 > 0$ by the bipolaronic mechanism of superconductivity in BPB. The inapplicability of this mechanism here is supported by the relative smallness [267] of the electron-phonon coupling constant $\lambda_{\text{el-ph}} < 1$, which rules out the strong coupling-induced $H_{c2}(T)$ modification [257] as well. Positive curvature is also present in the BPB's high- T_c relative BKB [49].

For hexagonal tungsten bronze Rb_xWO_3 , the positive curvature of $H_{c2}(T)$ and large values of $H_{c2}(0)$ are observed precisely for partially dielectrized compositions [56]. In agreement with our theory, $d^2H_{c2}/dT^2 > 0$ for quasi-2D purple bronze $\text{Li}_{0.9}\text{Mo}_6\text{O}_{17}$ [270].

High- T_c oxides usually exhibit a divergence of H_{c2} for decreasing T with a noticeable positive curvature in the neighborhood of T_c . For example, one should mention LSCO [236,271], YBCO [272], $\text{YBa}_2(\text{Cu}_{1-x}\text{Zn}_x)_3\text{O}_{7-y}$ [273], $\text{Bi}_2\text{Sr}_2\text{CuO}_y$ [274], $\text{Tl}_2\text{Ba}_2\text{CuO}_6$ [275], and $\text{Sm}_{1.85}\text{Ce}_{0.15}\text{CuO}_{4-y}$ [276]. In this connection, it is necessary to bear in mind that the anomalous vortex behavior in quasi-2D short-coherence length cuprates may drastically influence the very process of H_{c2} determination, making the proposed classical picture oversimplified [277].

Among the superconductors with $d^2H_{c2}/dT^2 > 0$ there are layered group-V transition-metal dichalcogenides such as $2H\text{-TaS}_2$ intercalated by various organic compounds [252,278], $4H\text{-TaS}_{1.6}\text{Se}_{0.4}(\text{collidine})_{1/6}$ [278], $2H\text{-NbS}_2$ [279], and $2H\text{-}$ and $4H\text{-Nb}_{1-x}\text{Ta}_x\text{Se}_2$ [280]. The superconducting properties of such systems are described by the Klemm–Luther–Beasley (KLB) theory [256], based on the idea of a Josephson coupling between layers. However, the KLB theory does not explain

the positive curvature of $H_{c2\perp}(T)$ (when the field is normal to layers), which practically always accompanies the positive curvature of $H_{c2\parallel}(T)$ [252,281]. The experimentally determined inflection point T^* of the $H_{c2\parallel}(T)$ dependence does not necessarily coincide [281] with T_{KLB}^* calculated from the condition of equality of the vortex core radius and the inter-layer distance. It raises doubts for the applicability of the KLB theory also in those cases when an analysis of the inflection-point location was not carried out.

Positive curvature of H_{c2} is inherent to $Tl_2Mo_6Se_6$ [79], quasi-1D partially gapped $NbSe_3$ [282], and ternary molybdenum chalcogenides (Chevrel phases) such as $EuMo_6S_8$ under pressure [255], $La_{1.2-x}Eu_xMo_6S_8$ [283], $Sn_xEu_{1.2-x}Mo_6S_8$ [284], and $SnMo_6S_8$ and $PbMo_xS_8$ (with $x = 6.00, 6.20, 6.35$) [285]. The experimental situation in Chevrel compounds is rather complicated. For $SnMo_6S_8$ and $PbMo_xS_8$ [285], without rare-earth ions, our interpretation seems unambiguous. In substances with Eu ions [255], the compensatory effect of Jaccarino and Peter plays a crucial role. It was proved in famous experiments [286] where the magnetic field-induced superconductivity of $Eu_{0.75}Sn_{0.25}Mo_6S_{7.2}Se_{0.8}$ was discovered.

As for the SDW superconductors, the positive $H_{c2}(T)$ curvature is observed, in heavy-fermion superconductor URu_2Si_2 [112,113,117], U_6Fe [287], $Cr_{1-x}Re_x$ [288], and organic superconductors: β -(ET) $_2I_3$ [289], κ -(ET) $_2Cu$ (CNS) $_2$ [107], (TMTSF) $_2ClO_4$ at ambient pressure [290], (TMTSF) $_2PF_6$ [291] and (TMTSF) $_2AsF_6$ [292] under external pressure. It is significant that in the alloy $Cr_{78}Re_{22}$ the positive sign of the curvature d^2H_{c2}/dT^2 becomes negative after annealing [288]. The width of the superconducting transition does not change in this case and $H_{c2}(0)$ decreases, which implies a reduction of the microscopic defect concentration n_i in the sample. These facts are also properly described in our theory. Indeed, the diffusion coefficients D_d and D_{nd} increase as n_i^{-1} and, according to Eq. (32), the quantity A , which determines the sign of the curvature, decreases in the same manner.

6. Josephson effect

6.1. Green's functions

Hereafter we consider pure DW superconductors in the absence of an external magnetic field. The normal $\mathcal{G}_{ij}^{\alpha\beta}(\mathbf{p}; \omega_n)$ and anomalous $\mathcal{F}_{ij}^{\alpha\beta}(\mathbf{p}; \omega_n)$ Matsubara GF's corresponding to the Hamiltonian (11) can be found from the Dyson–Gor'kov equations

(12) and (13). They are matrices in the space which is the direct product of the spin space and the isotopic space of the FS sections [16,17,20]. As in the previous Sections, we confine ourselves to the case $|\Sigma| \gg T_c$ and, hence, to the temperature range $0 < T < T_c \ll T_d(T_N)$. Owing to the symmetry of the problem, only the following different GF's are in action: $\mathcal{F}_{11}^{\alpha\beta} = \mathcal{F}_{22}^{\alpha\beta}$, $\mathcal{F}_{12}^{\alpha\beta} = \mathcal{F}_{21}^{\alpha\beta}$, $\mathcal{F}_{33}^{\alpha\beta}$, $\mathcal{G}_{11}^{\alpha\beta} = \mathcal{G}_{22}^{\alpha\beta}$, $\mathcal{G}_{12}^{\alpha\beta} = \mathcal{G}_{21}^{\alpha\beta}$, and $\mathcal{G}_{33}^{\alpha\beta}$. GF's with subscripts 12 and 21 correspond to the pairing from different nested FS sections. Explicit expressions for these functions can be found elsewhere [17,293,294].

6.2. Tunnel currents

To calculate the total tunnel current I through the junction we use the conventional approach [295] based on the tunnel Hamiltonian

$$\mathcal{H}_{\text{tun}} = \mathcal{H} + \mathcal{H}' + \mathcal{T}. \quad (34)$$

The left- and right-hand electrodes of the junction are described in Eq. (34) by the terms \mathcal{H} and \mathcal{H}' , respectively, which coincide with the Hamiltonian (11) with an accuracy up to notation. Hereafter the primed entities including sub- and superscripts correspond to the right-hand side of the junction. The tunnel term \mathcal{T} has the form

$$\mathcal{T} = \sum_{i,i'=1}^3 \sum_{\mathbf{p}\mathbf{q}\alpha} T_{\mathbf{p}\mathbf{q}}^{ii'} a_{i\mathbf{p}\alpha}^+ a_{i'\mathbf{q}\alpha} + \text{h.c.}, \quad (35)$$

where $T_{\mathbf{p}\mathbf{q}}^{ii'}$ are the tunnel matrix elements. We assume that all matrix elements $T^{ii'}$ are equal and not influenced by the existence of the superconducting and dielectric gaps, so that

$$T^{ii'} T^{jj'*} = \text{const} = |T|^2. \quad (36)$$

This approximation is analogous to the neglect of the influence of the gap Δ on $|T|^2$ in the standard Ambegaokar–Baratoff approach. Our assumption is natural in the framework of the BCS-type scheme, i.e., in the case of a weak coupling for Cooper and zero-channel pairings. The weak coupling approach is valid for the latter if the inequality $E_F \gg |\Sigma|$ holds. Then we can introduce the universal resistance R of the tunnel junction in the normal state

$$R^{-1} = 4\pi e^2 N(0) N'(0) \langle |T|^2 \rangle_{FS}, \quad (37)$$

where $N(0)$ and $N'(0)$ are the total electron DOS's for the metals on the left- and right-hand-sides [see Eq. (24)]. The angle brackets $\langle \dots \rangle_{FS}$ in equation

(37) imply averaging over the FS. In so doing it is assumed that the Fermi momentum k_F is the same for the d and nd sections of the FS for each superconductor [15–18].

6.3. Stationary Josephson effect (critical current)

Calculations of the critical Josephson current I_c across a symmetrical junction between DW superconductors were made in Ref. 226. In line with the BCS case, we have

$$I_c(T) = 4eT \sum_{i,i'} \sum_{pq} |T_{pq}|^2 \sum_{\omega_n} \mathcal{F}_i(\mathbf{p}; \omega_n) \mathcal{F}_{i'}(\mathbf{q}; -\omega_n), \quad (38)$$

where the outer summation is carried out over all relevant GF's. The intersection GF's \mathcal{F}_{12} enter into this expression only in the SDW case [226]. The calculations, using approximations (36) and (37), show that the dimensionless dependences of the ratio $I_c(T)/I_c(T=0)$ on the dimensionless temperature $\theta = T/T_c$, similarly to the dependences of $\Delta(T)/\Delta(0)$ on θ (see Sec. 4.1), do not deviate significantly from the Ambegaokar–Baratoff curve in the case of both CDW and SDW superconductors. Again, the amplitude $I_c(0)$ depends drastically on the magnitude of the dielectric OP Σ and the degree of dielectrization ν of the FS.

6.4. Nonstationary Josephson effect (theory)

In the adiabatic approximation $V^{-1} dV/d\tau \ll \ll T_c$, when the ac bias voltage $V(\tau) \equiv V_{\text{right}}(\tau) - V_{\text{left}}(\tau)$ across the Josephson junction varies adiabatically slowly in comparison with energies of the order of T_c and τ is the time, we obtain a nine-term expression for I [293,294], which is a generalization of that for the BCS-superconductor case [295]

$$I[V(\tau)] = \sum_{i,i'} [I_{(i,i')}^1(V) \sin 2\varphi + I_{(i,i')}^2(V) \cos 2\varphi + J_{(i,i')}], \quad (39)$$

where $\varphi = \int eV(\tau) d\tau$; I^1 is the Josephson current amplitude; I^2 is the interference pair-quasiparticle current amplitude; and J is the quasiparticle current. The subscript (i, i') means the combination of GF's (only \mathcal{F} s for $I^{1,2}$ and only \mathcal{G} s for J) needed to calculate the term. Thus, since $\mathcal{F}_{12} = 0$ in the CDW case, the number of relevant terms for $I^{1,2}$ decreases. Below, in accordance with the most representative experimental setups, we confine ourselves to junctions made up of identical SDW or CDW superconductors on both sides or to the case

when a DW superconductor serves as one electrode and a BCS superconductor is the other one.

It is obvious that the tunnel current-voltage characteristics (CVC's) for CDW superconductors would be more complex than in the BCS case. This is so because the positions of CVC anomalies (logarithmic singularities or jumps) are defined by a sum of or a difference between the relevant poles of the GF's $\mathcal{F}(\omega)$ and $\mathcal{G}(\omega)$ contained in the expressions for $I_{(i,i')}^{1,2}$ and $J_{(i,i')}$. For a BCS superconductor there is only one pole at $\omega = \Delta_{BCS}$, and for a CDW superconductor the poles are at $\omega = \Delta$ and $\omega = D$ [see Eq. (27)], the «combined effective gap». For SDW superconductors the situation is even more involved, since there are two «combined effective gaps» $|D_{\pm}|$ [see Eq. (28)].

The phases φ and φ' of the superconducting order parameters are free [296], with their difference $\varphi_{\text{diff}} = \varphi' - \varphi$ obeying the above Josephson relationship linking it to the bias voltage. On the contrary, we assume a strong DW pinning by lattice defects or impurities, so their phases χ and χ' on each side of the junction are fixed. In the absence of pinning the phase of the DW (and consequently the phase χ of the OP $\Sigma \equiv |\Sigma| e^{i\chi}$) is arbitrary [5,9]. This fact leads, in particular, to collective-mode conductivity [9].

Pinning prevents DW sliding in quasi-1D compounds for small electric fields, whereas for large ones various coherent phenomena resembling the Josephson effect, e.g., Shapiro steps on the CVC's, become possible [5,9]. For excitonic insulators the behavior is more complicated. In particular, the phase χ is fixed by the Coulomb interband matrix elements (which link FS sections 1 and 2) corresponding to two-particle transitions V_2 and by the interband electron-phonon interaction described by the constant $\lambda_{\text{el-ph}}$ [7,8,12,222]. Moreover, the excitonic transitions due to the finite values of V_2 and $\lambda_{\text{el-ph}}$ are always first-order, although close to second-order, transitions [222]. The contribution from the single-particle Coulomb interband matrix elements V_3 , which connect three particles from, say, FS section 1 and one particle from FS section 2, or vice versa, results in even more radical consequences. Namely, the self-consistency equation for the OP Σ becomes inhomogeneous, with the right-hand side proportional to V_3 . This leads to fixation of the phase χ [297]. On the other hand, if the causes of phase fixation are absent (e.g., for large applied electrostatic fields), the quasiparticle current between two Peierls insulators involves a term proportional to $\cos(\chi' - \chi)$ [221]. These phenomena are left beyond the scope of the review. However,

even in the present case of fixed χ two possibilities remain open for Σ : its sign may be either positive or negative, which affects the shape of the CVC's for tunnel junctions [205].

As a consequence, the terms for current amplitudes can be separated into two groups which are different in symmetry when the bias voltage V changes its polarity. Namely, there are terms possessing the usual properties:

$$I_{(i,i')}^{1,2}(-V) = \pm I_{(i,i')}^{1,2}(V), \quad J_{(i,i')}(-V) = -J_{(i,i)}(V), \quad (40)$$

where the upper and lower signs correspond to the Josephson and interference current amplitudes, respectively. At the same time, there are also terms with opposite symmetry relations:

$$I_{(i,i')}^{1,2}(-V) = \mp I_{(i,i')}^{1,2}(V), \quad J_{(i,i')}(-V) = J_{(i,i)}(V). \quad (41)$$

The expressions for these terms include products of the 12 GF's for one electrode and 11 or 33 GF's for the other one. Therefore, for nonsymmetrical (ns) junctions composed of different SDW superconductors (or an SDW superconductor and a BCS superconductor) all three current amplitudes $I_{ns}^{1,2}$ and J_{ns} are asymmetrical with respect to the bias voltage polarity, contrary to the well-known symmetrical form of CVC's for ns junctions involving different BCS superconductors. Since for CDW superconductors $\mathcal{F}_{12} = 0$, the CVC asymmetry occurs in this case only for the quasiparticle current J_{ns} .

We should point out that there may be also several other possible reasons leading to the quasiparticle CVC asymmetry for junctions involving normal metals as well as superconductors: (i) the imperfect nesting for SDW's due to the 3D warping of the FS [298], (ii) the electron-hole asymmetry of the primordial one-particle spectrum [299], (iii) existence of the submerged band of nondegenerate fermions [300], (iv) noncoincidence of the Fermi energy and the Van Hove singularity in the Van Hove scenario of superconductivity [209], (v) the directional tunneling, when the matrix elements $T_{pq}^{ii'}$ depend on quasimomenta and the band structure [301], (vi) the simultaneous involvement of polaron and bipolaron bands [204] or a bipolaron transfer into polarons in the related scenario [302], and (vii) a new phenomenon of symmetry breaking in symmetrical tunnel junctions predicted by us [207,303].

Tunnel junctions between two identical DW superconductors are even more interesting. In fact,

the ground state of a DW superconductor is degenerate with respect to the sign of the dielectric OP Σ (see Sec. 4). Therefore, there may exist two different states of the tunnel junction between *thermodynamically equivalent* DW superconductors. Both of them are characterized by $\Delta = \Delta'$ and $\nu = \nu'$, but for the one state $\Sigma = \Sigma'$ and for the other $\Sigma = -\Sigma'$. The first state (realized in junctions $S_{\Sigma} I S_{\Sigma}$ or $S_{-\Sigma} I S_{-\Sigma}$) is a genuinely symmetrical, *s*, state, whereas the broken symmetry, *bs*, is inherent to the other possible states (junctions $S_{\Sigma} I S_{-\Sigma}$ (*bs+* state) or $S_{-\Sigma} I S_{\Sigma}$ (*bs-* state)). In principle, *bs*

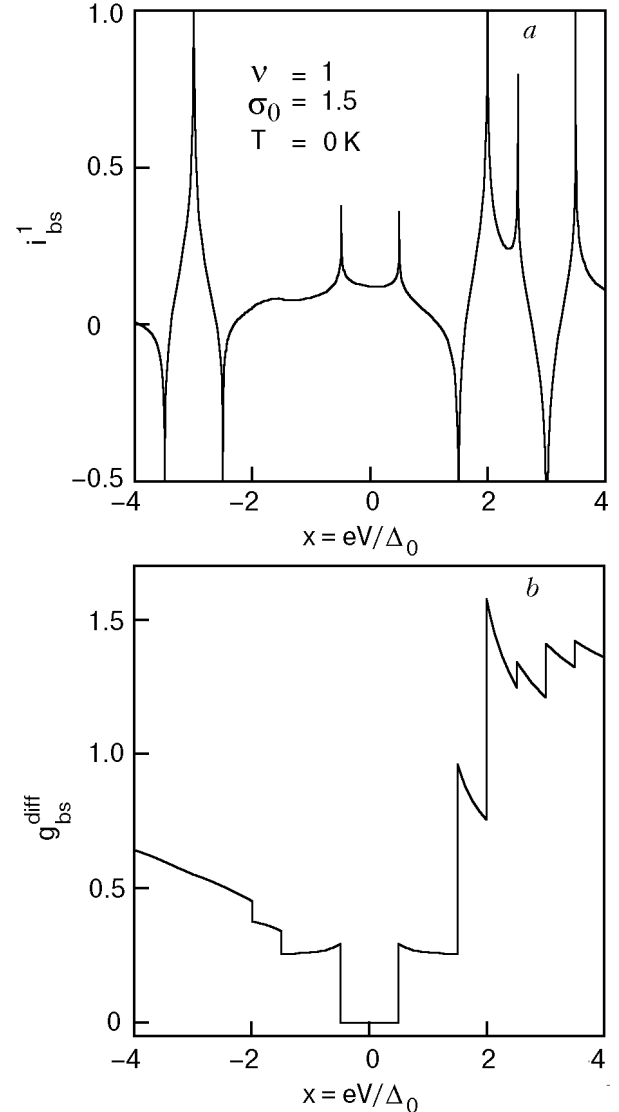


Fig. 5. Dimensionless current-voltage characteristics (CVC) of nonstationary Josephson current through the symmetrical $S_{\Sigma}^{SDW} I S_{-\Sigma}^{SDW}$ tunnel junction with broken symmetry (*bs+* state, see explanations in the text). Here $i_{bs}^1 = I_{bs}^1 eR/\Delta_0$, I_{bs}^1 is the current amplitude, e is the elementary charge, R is the junction resistance in the normal state, V is the bias voltage, Δ_0 is the superconducting order parameter at $T = 0$ in the absence of the FS dielectrization (a). The dimensionless quasiparticle conductance $g_{bs}^{diff} = R dJ_{bs}/dV$, (J_{bs} is the quasiparticle current) (b).

junctions are nonsymmetrical and, hence, exhibit nonsymmetrical CVC's similarly to their *ns* counterparts. Figure 5 demonstrates a set of theoretical curves calculated for the tunnel junction between identical SDW superconductors when the symmetry of the junction is broken (in the *bs+* state of the junction). The CVC asymmetry for the *bs* junctions, as in the *ns* case, is driven by the unconventional structure of the functions $\mathcal{F}_{12}(\omega)$ and $\mathcal{G}_{12}(\omega)$. Analogously to the *ns* case, the symmetry breaking for CDW superconductors may occur only for the quasiparticle current $J_{bs}(V)$ [207,303].

The situation concerned is quite similar to that for many-body systems with broken symmetry. The existence of two electrically connected pieces of DW superconductors makes the symmetry breaking *macroscopically observable*. Fluctuations act here as a driving force promoting selection between various possible states. Thus we obtain for a formally symmetrical junction a discrete set of states corresponding to various possible combinations of the sign of the dielectric OP in the electrodes. The statistical weight of the *s* state is twice that for each of the *bs* states.

6.5. Discussion and comparison with experiment

6.5.1. CDW superconductors

The results presented above are of a quite general character due to the phenomenological nature of our approach. The main obstacle that makes it difficult to make direct predictions for specific compounds is the absence of reliable estimates for the parameters. This especially concerns the gapped FS fraction described by ν . The rare exception is the quasi-1D substance NbSe₃ (see Table 1). But calculations [207,293] show that the extremely high ratio $T_d/T_c \approx 50$ in this substance is unfavorable for experimental observation of the predicted interplay between Δ and Σ in the CVC's. The more suitable object for such measurements seems to be the layered compound 2H-NbSe₂. Of course, the study of other partially gapped CDW superconductors would be also helpful for discovering multiple-gap structure in Josephson and quasiparticle CVC's. Indeed, the discussion given below shows the CDW features might have been revealed in quasiparticle TS and PCS measurements for NbSe₃ and different oxides.

In particular, the asymmetrical experimental dependence $G^{\text{diff}}(V)$ for NbSe₃ in the normal state [44] reflects the main features of our theory [207,303]. The alternative description given in

Ref. 44 is based on a model [298] with imperfect nesting, predicting that the interchain hopping matrix element, combined with Σ into linear combinations, determines the CVC anomalies. The choice between two models concerned would have been most easily made while studying the superconducting state. The asymmetry of CVC's for junctions involving NbSe₃ was also observed in Ref. 42.

The available experimental data on the peculiarities of the quasiparticle currents through BPB-based junctions are contradictory. According to Ref. 304, the gap edge voltage grows with increasing x and reaches the level V_{up} at $x \geq 0.2$, for which the ratio V_{up}/T_c is equal to the BCS weak-coupling value $\Delta(T=0)/T_c = \pi/\gamma$ [3]. On the other hand, in the BPB with $x = 0.25$ gap features appear in the bias range 60–100 K of tunnel characteristics, depending on the sample and the estimation method [305]. However, the T_c in Refs. 304,305 virtually coincide. The results of Ref. 305 can be understood on the basis of our theory. In this case the smaller gap Δ_{min} is likely to be indiscernible against the background of the larger one Δ_{max} . This could be associated with a smearing of the anomaly corresponding to the dielectric gap $\Sigma \equiv \Delta_{\text{max}}$ due to the averaging of the contributions to the total current $J(V)$ from areas with different Σ . A possible source of the spread in Σ magnitudes may be the chemical inhomogeneities of the grain boundaries mentioned above [14]. Nevertheless, the question is far from a final answer. Nonlinearities of point-contact CVC's at much larger voltages $eV \approx 10^3$ K were claimed to be observed for BPB with $x = 0.25$ [306]. We think that the authors were correct in supposing that the effect was linked to the CDW existence. But the gap value $\Sigma \approx 10^3$ K assumed by them does not follow actually from the measurements. It stems merely from an attempt to correlate their point-contact results with the optical data [92]. At the same time, a pronounced nonlinearity of G_s^{diff} for BPB, according to our point of view, should be observed at $eV \approx 100$ meV, since $\Sigma \approx 50$ –100 K.

In tunnel CVC's of superconducting BKB samples only one gap feature was revealed [307]. In order to reconcile these data with the evidence of the Σ and Δ coexistence [64–66], one may adopt the hypothesis [65] of the percolative nature of the noncubic semiconducting BKB phase in the bulk superconducting crystals. The quest for the multiple-gap structure is to be continued because its apparent absence may in reality result from small magnitudes. However, the asymmetry of CVC's for *ns* junctions [308] favors our interpretation.

TS, PCS, and STM have been used since the discovery of high- T_c superconductivity to elucidate its nature. The results proved to deviate substantially from the quasiparticle CVC's in the framework of the BCS theory [295]. Unfortunately, the gap values extracted from conductivities G^{diff} differ for the same substance when measured by various groups [309,310]. This undesirable situation may be due not only to the poor quality of the samples and junctions but also to intrinsic phenomena in oxides connected to their thermal history [14] or to sample heating, which can be avoided by the short-pulse technique [311].

The main unconventional properties that are often present in different cuprates include a two- or even multiple-gap CVC structure both for s and ns junctions as well as CVC asymmetry for ns junctions. Thus, two-gap behavior is seen in the point-contact CVC of LSCO [310] and in the tunnel CVC's for s (or ns) break junctions involving this oxide [312]. The extra dip or dip-hump features are commonly observed for both voltage polarities in s junctions or for one polarity in ns junctions, which involve $\text{HgBa}_2\text{Ca}_2\text{Cu}_3\text{O}_{8-y}$ (PCS) [313] and $\text{HgBa}_2\text{Ca}_{n-1}\text{Cu}_n\text{O}_{2n+2+y}$ with $n = 1, 2, 3$ (TS) [301], YBCO (TS) [314], $\text{YbBa}_2\text{Cu}_3\text{O}_{7-y}$ (TS) [314], and $\text{YBa}_2(\text{Cu}_{1-y}\text{Zn}_y)_3\text{O}_7$ (PCS) [315].

For BSCCO-based tunnel junctions many experiments have revealed a «pseudogap» persisting above T_c [316–319] and smoothly evolving into Δ below T_c [317,318], but sometimes coexisting with Δ [319]. Unfortunately, there is a disagreement whether the pseudogap manifests itself only in underdoped samples [318] or also in overdoped ones [317]. The STM method has even made it possible to trace the (pseudogap-related?) influence of CDW's on the electronic DOS for Bi–O semiconducting planes [320].

In the superconducting state of BSCCO, tunnel measurements in the ns setup often show a dip (with a magnitude of about 10% of the peak height) at about $V \approx -2\Delta/e$ [317], whereas for s junctions the dips (or dip-hump structures) are observed at $V \approx \pm 3\Delta/e$ [321]. A thorough analysis of tunneling data [322] led the author to the conclusion that the CVC's for BSCCO exhibit, in reality, 4 gaps: dielectric, superconducting isotropic spinon, superconducting magnetic polaron with $d_{x^2-y^2}$ symmetry, and small superconducting with g -wave symmetry. In this case it was not the partial-gapping but the phase-separation scenario that was adopted. It seems premature to discuss the latter results, which are not yet confirmed by other groups.

In view of the existence of an asymmetrical dip, it is hardly surprising that the overall CVC patterns for ns junctions with BSCCO electrodes are also asymmetrical (including the superconducting peak heights of $G_{ns}^{\text{diff}}(V)$) [317,318,321]. Asymmetrical CVC's in the ns case have also been observed for YBCO in TS and PCS experiments [314], for Hg-based oxides [301,313], LSCO [312], and combined YBCO– I – $\text{HoBa}_2\text{Cu}_3\text{O}_{7-x}$ junctions [323].

The dependences $G_{ns}^{\text{diff}}(V)$ for ns junctions with BSCCO are shown as typical examples of asymmetrical patterns in Fig. 6. The major features of these curves are reproduced by our theory. The dip voltages V_{ns}^{dip} should be identified with D/e , bearing in mind the data which support the existence of CDW's in cuprates (see Sec. 2). For the reasonable assumption $\Sigma \approx \Delta\sqrt{3}$ one obtains $eV_{ns}^{\text{dip}} \approx 2\Delta$, in accordance with the experiment. On the other hand, according to our theory, for s -junctions the smaller extra singular point of $J_s(V)$ and $G_s^{\text{diff}}(V)$ is $eV_s^{\text{dip}} = \Delta + D$. Then the same chosen ratio $\Sigma/\Delta = \sqrt{3}$ leads to $eV_s^{\text{dip}} = 3\Delta$, which exactly matches the experimental values [321]. As to the larger singularity at $eV = 2D$, its calculated amplitude is much smaller. Making allowance for the inevitable

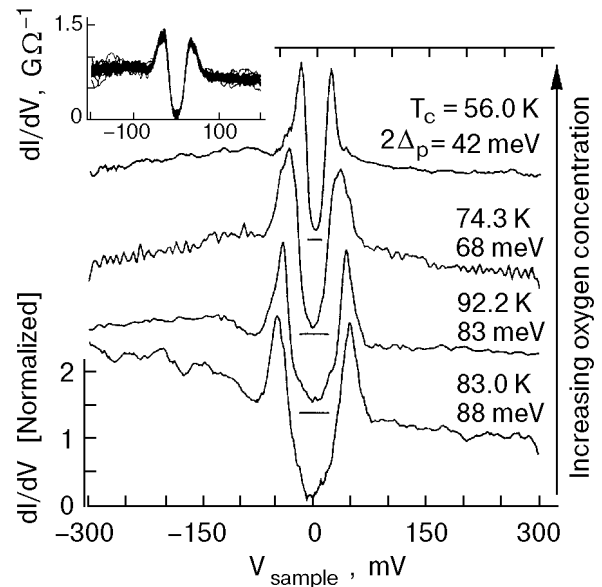


Fig. 6. Tunneling spectra for BSCCO measured at 4.2 K for different oxygen doping levels. The curves are normalized to the conductance at 200 mV and offset vertically for clarity (zero conductance is indicated for each spectrum by the horizontal line at zero bias). The estimated error on the gap values ($2\Delta_p$) is ± 4 meV. The inset shows 200 superposed spectra measured at equally spaced points along a $0.15 \mu\text{m}$ line on overdoped BSCCO ($T_c = 71.4$ K), demonstrating the spatial reproducibility (from Ref. 317).

CVC smearing [324], one should expect that the singularity considered is invisible.

Most of the tunnel experiments for the electron-doped oxide $\text{Nd}_{1.85}\text{Ce}_{0.15}\text{CuO}_{4-x}$ demonstrate the conventional quasiparticle CVC's [325,326]. Only $G_s^{\text{diff}}(V)$ obtained in Ref. 325 reveals the one-polarity dip at $eV \approx 2\Delta$ for the *symmetrical* setup. It seems quite plausible that in these experiments the *bs*-regime predicted earlier [207,303] is achieved.

It should be noted that the dielectrization concept survives for arbitrary superconducting gap symmetry [327], thus preserving almost unaltered our interpretation of the experimental data.

In addition to our point of view and the $d_{x^2-y^2}$ interpretation of the $G^{\text{diff}}(V)$ fine structure in cuprates [328], one should mention the *s*-wave two-gap *SN* layered model and the related one which takes into account the surface Δ modification [329]. Another two-gap possibility for the superconducting DOS was presented in Ref. 330 on the basis of the anisotropic *s*-wave gap function $\Delta(\varphi) = \Delta_1 + \Delta_2 \cos 4\varphi$. The corresponding DOS feature points are $|\Delta_1 - \Delta_2|$ and $\Delta_1 + \Delta_2$. There was also an attempt [328] to describe the above-mentioned dips in $G^{\text{diff}}(V)$ by the strong-coupling multiboson emission. This speculation was rejected by the *d*-wave adherents [331] on the basis of the too small magnitude of the strong-coupling-induced peculiarities.

So far, only the quasiparticle currents $J(V)$ were discussed. We are not aware of any nonstationary Josephson current $I^1(V)$ measurements for high- T_c oxides with the aim of observing the Riedel singularity. The latter was found, however, in BSCCO as a by-product of the Raman-active optical phonon detection by the $J(V)$ current branch [332]. These phonons were generated by the Josephson current, and the emission intensity strongly decreased after the specific phonon frequencies exceeded the Riedel values $4\Delta(T)$. It is natural to suggest that the extra Riedel singularities $\Delta + D$ and $2D$ (in the *s* and *bs* cases) or $D + \Delta_{BCS}$ (in the *ns* case) [207,293], although expected to be less vigorous, can be detected in the same manner as in Ref. 332. The confirmation of the dielectrization influence on $I^1(V)$ would be the *experimentum crucis* for the adopted underlying concept and may also result in practical benefits, since $|\Sigma|$ is usually much larger than Δ .

6.5.2. SDW superconductors

Heavy-fermion SDW superconducting compounds are the most probable objects to be described by the presented scheme involving FS partial gapping. For instance, tunnel CVC's are *asymmetrical* for break junctions (symmetrical in

essence!) made of superconducting UNi_2Al_3 [333]. This is reconciled with our theory. However, the situation may turn out more complex. In fact, subsequent PCS investigations for UNi_2Al_3 revealed *no* clear-cut gap features, whereas peaks at SDW gap edges do exist in the related compound UPd_2Al_3 and vanish above T_N [131]. At the same time, the noticeable *V*-like falloff near zero bias for $[G_s^{\text{diff}}(V)]^{-1}$ of UNi_2Al_3 is explained by self-heating effects [131].

The compound URu_2Si_2 is a relatively thoroughly studied partially dielectrized superconductor. There are, however, substantial discrepancies for the parameters Σ and v (see Table 2). TS and PCS measurements of URu_2Si_2 conductivity both in the *s* and *ns* setup have been carried out recently [109,115,119,125]. The respective CVC's clearly demonstrated gap-like peculiarities disappearing above T_N , thus being the manifestation of the SDW-related partial dielectric gapping. Below T_c , superconducting gap features were also seen at voltages associated with T_c 's by the BCS relationship. Usually, such experiments give an opportunity to obtain the 2Σ value directly as the voltage difference between two humps (tunnel method), or valleys (point-contact technique) of the curves $G^{\text{diff}}(V)$. However, in this case the CVC's for junctions URu_2Si_2 *IM* or URu_2Si_2 *CM*, where *C* denotes a constriction, are highly nonsymmetrical. It agrees qualitatively with our theory, but a quantitative comparison is difficult. Direct tunnel or point-contact studies lead to strikingly different values of Σ as compared to the value cited above, e.g., $\Sigma \approx 68$ K [115,119].

It also turned out that the broken symmetry scenario has already been realized for URu_2Si_2 point homocontacts [119]. In agreement with our theory, the CVC asymmetry is smaller for homocontacts than for heterocontacts. Moreover, together with symmetrical CVC's, it often happens that the Σ -determined anomalies of the experimental dV/dJ curves are more pronounced either on the positive, or negative *V*-branches. It correlates well with our classification of formally symmetrical junctions as of the *s*, *bs+*, or *bs-* types.

We should note that the cited tunnel and point-contact measurements for junctions involving URu_2Si_2 were carried out for single crystals, whereas our procedure of summation of all possible tunnel currents between different FS sections implies a certain directional averaging. However, the gap features and the general appearance, e.g., of the dV/dJ vs. *V* dependences [119], are very similar for directions along the *c* axis or normal to it. This

is so because some kind of averaging is inevitably present in such experiments. In this manner, our approach is reconciled with the experimental data.

Conclusions

A great body of information analyzed in this review indicates the existence of common features for different classes of superconducting substances. It is shown that they can be adequately described in the framework of the partial electron spectrum dielectrization concept. The competition between Cooper pairing and various instabilities resulting in other collective states, including DW's, is likely to constrain the maximum possible T_c . On the other hand, the combined phase where DW's and Cooper pairing coexist gives rise to a great many of new interesting phenomena regardless of the background microscopic instability mechanisms. Further theoretical and experimental investigations will undoubtedly enhance the number of such phenomena and provide us with their proper explanations.

Acknowledgments

We are grateful to all our Ukrainian and foreign colleagues with whom we discussed the topics of this review and who sent us pre- and reprints of their works. Missions of A. G. to Northeastern University (Boston) sponsored by NATO and of A. V. to NIST (Gaithersburg) sponsored by CRDF were very helpful. In this connection the cooperation with R. S. Markiewicz and J. W. Gadzuk is highly appreciated. We are also grateful to INTAS (project 94-3862 under the direction of R. I. Shekhter and M. Jonson (Göteborg)) for financial sponsorship and to M. Ausloos (Liege) for big help in the dissemination of our results. We express our thanks to O. V. Dolgov (Tübingen) for valuable information as well as to the V. I. Vernadsky National Library of Ukraine and INTAS program IA-98-01 for bibliographic assistance. This work was supported in part by the Ukrainian State Foundation for Fundamental Research (grant 2.4/100).

1. R. E. Peierls, *Quantum Theory of Solids*, Clarendon Press, Oxford (1955).
2. H. Fröhlich, *Proc. Roy. Soc. London* **A223**, 296 (1954).
3. A. A. Abrikosov, L. P. Gor'kov, and I. E. Dzyaloshinskii, *Methods of Quantum Field Theory in Statistical Physics*, Prentice Hall, Englewood Cliffs, New York (1963).
4. L. B. Coleman, M. J. Cohen, D. J. Sandman, F. G. Yamagishi, A. F. Garito, and A. J. Heeger, *Solid State Commun.* **12**, 1125 (1973).
5. G. Grüner, *Rev. Mod. Phys.* **60**, 1129 (1988).
6. G. Rickayzen, *Essays in Physics* **3**, 1 (1971).

7. B. I. Halperin and T. M. Rice, *Solid State Phys.* **21**, 115 (1968).
8. Yu. V. Kopaev, *Trudy Fiz. Inst. Akad. Nauk SSSR* **86**, 3 (1975).
9. G. Grüner, *Rev. Mod. Phys.* **66**, 1 (1994).
10. E. Fawcett, H. L. Alberts, V. Yu. Galkin, D. R. Noakes, and J. V. Yakhmi, *Rev. Mod. Phys.* **66**, 25 (1994).
11. A. W. Overhauser, *Phys. Rev. Lett.* **4**, 462 (1960).
12. *Problems of High-Temperature Superconductivity*, V. L. Ginzburg and D. A. Kirzhnits (eds.), Nauka, Moscow (1977) (in Russian).
13. V. M. Pan, V. G. Prokhorov, and A. S. Shpigel, *Metal Physics of Superconductors*, Naukova Dumka, Kiev (1984), in Russian.
14. A. M. Gabovich and D. P. Moiseev, *Usp. Fiz. Nauk* **150**, 599 (1986).
15. A. M. Gabovich, A. S. Gerber, and A. S. Shpigel, *Phys. Status Solidi* **B141**, 575 (1987).
16. A. M. Gabovich and A. S. Shpigel, *Phys. Rev.* **B38**, 297 (1988).
17. A. M. Gabovich and A. S. Shpigel, *J. Phys.* **F14**, 3031 (1984).
18. G. Bilbro and W. L. McMillan, *Phys. Rev.* **B14**, 1887 (1976).
19. I. Eremin, M. Eremin, S. Varlamov, D. Brinkmann, M. Mali, and J. Roos, *Phys. Rev.* **B56**, 11305 (1997).
20. A. M. Gabovich and A. S. Shpigel, *Zh. Eksp. Teor. Fiz.* **84**, 694 (1983).
21. M. J. Nass, K. Levin, and G. S. Grest, *Phys. Rev.* **B25**, 4541 (1982).
22. K. Machida, *J. Phys. Soc. Jpn.* **50**, 2195 (1981).
23. A. I. Buzdin and L. N. Bulaevskii, *Usp. Fiz. Nauk* **144**, 415 (1984).
24. H. Won and K. Maki, in: *Symmetry and Pairing in Superconductors*, M. Ausloos and S. Kruchinin (eds.), Kluwer Academic, Dordrecht (1999), p. 3.
25. K. Bechgaard and D. Jérôme, *Physica Scripta* **T39**, 37 (1991).
26. D. Jérôme, C. Berthier, P. Molinié, and J. Rouxel, *J. Phys. (Paris) Colloq.* **4** **37**, C125 (1976).
27. L. N. Bulaevskii, *Usp. Fiz. Nauk* **116**, 449 (1975).
28. Yu. V. Kopaev and A. I. Rusinov, *Phys. Lett.* **A121**, 300 (1987).
29. M. Kato, Y. Suzumura, Y. Okabe, and K. Machida, *J. Phys. Soc. Jpn.* **57**, 726 (1988).
30. K. Machida and M. Kato, *Phys. Rev. Lett.* **58**, 1986 (1987).
31. V. L. Ginzburg and E. G. Maksimov, *Sverkhprovodimost* **5**, 1543 (1992).
32. A. S. Alexandrov and N. F. Mott, *Rep. Prog. Phys.* **57**, 1197 (1994).
33. V. M. Loktev, *Fiz. Nizk. Temp.* **22**, 3 (1996).
34. J. F. Annett, N. D. Goldenfeld, and A. J. Leggett, in: *Physical Properties of High Temperature Superconductors V*, D. M. Ginsberg (ed.), World Scientific, River Ridge, New York (1996), p. 375.
35. R. S. Markiewicz, *J. Phys. Chem. Sol.* **58**, 1179 (1997).
36. B. Brandow, *Phys. Rep.* **296**, 1 (1998).
37. J.-J. Kim, W. Yamaguchi, T. Hasegawa, and K. Kitazawa, *Phys. Rev.* **B50**, 4958 (1994).
38. W. Sachs, D. Roditchev, and J. Klein, *Phys. Rev.* **B57**, 13118 (1998).
39. A. Prodan, S. W. Hla, V. Marinković, H. Böhm, F. W. Boswell, and J. C. Bennett, *Phys. Rev.* **B57**, 6235 (1998).
40. I. B. Altfeder and S. V. Zaitsev-Zotov, *Phys. Rev.* **B54**, 7694 (1996).

41. H. L. Edwards, A. L. Barr, J. T. Markert, and A. L. de Lozanne, *Phys. Rev. Lett.* **73**, 1154 (1994).
42. T. Ekino and J. Akimitsu, *Physica* **B194–196**, 1221 (1994).
43. Z. Dai, C. G. Slough, and R. V. Coleman, *Phys. Rev.* **B45**, 9469 (1992).
44. J. P. Sorbier, H. Tortel, P. Monceau, and F. Lévy, *Phys. Rev. Lett.* **76**, 676 (1996).
45. C. Wang, B. Giambattista, C. G. Slough, R. V. Coleman, and M. A. Subramanian, *Phys. Rev.* **B42**, 8890 (1990).
46. C. Schlenker, C. Hess, C. Le Touze, and J. Dumas, *J. Phys. I (Paris)* **6**, 2061 (1996).
47. T. Ekino, J. Akimitsu, Y. Matsuda, and M. Sato, *Solid State Commun.* **63**, 41 (1987).
48. C.-H. Du and P. D. Hatton, *Europhys. Lett.* **31**, 145 (1995).
49. N. V. Anshukova, A. I. Golovashkin, L. I. Ivanova, O. T. Malyuchkov, and A. P. Rusakov, *Zh. Eksp. Teor. Fiz.* **108**, 2132 (1995).
50. E. Canadell and M.-H. Whangbo, *Int. J. Mod. Phys.* **B7**, 4005 (1993).
51. Y. Koyama and M. Ishimaru, *Phys. Rev.* **B45**, 9966 (1992).
52. Y. Koyama, S.-I. Nakamura, and Y. Inoue, *Phys. Rev.* **B46**, 9186 (1992).
53. Y. Bando and S. Iijima, *Acta Crystallogr.* **B37**, Suppl., C303 (1981).
54. L. H. Cadwell, R. C. Morris, and W. G. Moulton, *Phys. Rev.* **B23**, 2219 (1981).
55. M. Sato, B. H. Griever, G. Shirane, and H. Fujishita, *Phys. Rev.* **B25**, 501 (1982).
56. R. K. Stanley, R. C. Morris, and W. G. Moulton, *Phys. Rev.* **B20**, 1903 (1979).
57. S. Etemad, *Phys. Rev.* **B13**, 2254 (1976).
58. F. Denoyer, R. Comés, A. F. Garito, and A. J. Heeger, *Phys. Rev. Lett.* **35**, 445 (1975).
59. R. Comés, S. M. Shapiro, G. Shirane, A. F. Garito, and A. J. Heeger, *Phys. Rev. Lett.* **35**, 1518 (1975).
60. Th. Straub, R. Claessen, Th. Finteis, P. Steiner, S. Hüfner, C. S. Oglesby, and E. Bucher, *Physica* **B259–261**, 981 (1999).
61. P. Monceau, J. Peyrard, J. Richard, and P. Molinié, *Phys. Rev. Lett.* **39**, 161 (1977).
62. R. P. S. M. Lobo and F. Gervais, *Phys. Rev.* **B52**, 13294 (1995).
63. T. Hashimoto, R. Hirasawa, T. Yoshida, Y. Yonemura, J. Mizusaki, and H. Tagawa, *Phys. Rev.* **B51**, 576 (1995).
64. A. Yu. Ignatov, A. P. Menushenkov, and V. A. Chernov, *Physica* **C271**, 32 (1996).
65. A. V. Puchkov, T. Timusk, W. D. Mosley, and R. N. Shelton, *Phys. Rev.* **B50**, 4144 (1994).
66. W. D. Mosley, J. W. Dykes, R. N. Shelton, P. A. Sterne, and R. H. Howell, *Phys. Rev. Lett.* **73**, 1271 (1994).
67. K. H. Kim, C. U. Jung, T. W. Noh, and S. C. Kim, *Phys. Rev.* **B55**, 15393 (1997).
68. A. I. Liechtenstein, I. I. Mazin, C. O. Rodriguez, O. Jepsen, O. K. Andersen, and M. Methfessel, *Phys. Rev.* **B44**, 5388 (1991).
69. M. R. Skokan, W. G. Moulton, and R. C. Morris, *Phys. Rev.* **B20**, 3670 (1979).
70. H. R. Shanks, *Solid State Commun.* **15**, 753 (1974).
71. S. Reich and Y. Tsabba, *Eur. Phys. J.* **B** (1999), to be published.
72. A. García-Ruiz and Bokhimi, *Physica* **C204**, 79 (1992).
73. C. Hess, C. Schlenker, G. Bonfait, J. Marcus, T. Ohm, C. Paulsen, J. Dumas, J.-L. Tholence, M. Greenblatt, and M. Almeida, *Physica* **C282–287**, 955 (1997).
74. K. Kawabata, *J. Phys. Soc. Jpn.* **54**, 762 (1985).
75. C. A. Swenson, R. N. Shelton, P. Klavins, and H. D. Yang, *Phys. Rev.* **B43**, 7668 (1991).
76. H. D. Yang, P. Klavins, and R. N. Shelton, *Phys. Rev.* **B43**, 7676 (1991).
77. H. D. Yang, P. Klavins, and R. N. Shelton, *Phys. Rev.* **B43**, 7681 (1991).
78. H. D. Yang, P. Klavins, and R. N. Shelton, *Phys. Rev.* **B43**, 7688 (1991).
79. R. Brusetti, A. Briggs, O. Laborde, M. Potel, and P. Gougeon, *Phys. Rev.* **B49**, 8931 (1994).
80. R. C. Lacoé, S. A. Wolf, P. M. Chaikin, C. Y. Huang, and H. L. Luo, *Phys. Rev. Lett.* **48**, 1212 (1982).
81. H. Takei, M. Yamawaki, A. Oota, and S. Noguchi, *J. Phys.* **F15**, 2333 (1985).
82. L. Brossard, M. Ribault, L. Valade, and P. Cassoux, *Phys. Rev.* **B42**, 3935 (1990).
83. N. A. Fortune, K. Murata, M. Ishibashi, M. Tokumoto, N. Kinoshita, and H. Anzai, *Solid State Commun.* **77**, 265 (1991).
84. R. H. Friend and D. Jérôme, *J. Phys.* **C12**, 1441 (1979).
85. S. I. Vedenev, A. I. Golovashkin, I. S. Levchenko, and G. P. Motulevich, *Zh. Eksp. Teor. Fiz.* **63**, 1010 (1972).
86. H. J. Levinstein and J. E. Kunzler, *Phys. Lett.* **20**, 581 (1966).
87. L. Y. L. Shen, *Phys. Rev. Lett.* **29**, 1082 (1972).
88. V. A. Finkel, *Structure of Superconducting Compounds*, Metallurgiya, Moscow (1983), (in Russian).
89. M. Greenblatt, W. H. McCarroll, R. Neifield, M. Croft, and J. V. Waszczak, *Solid State Commun.* **51**, 671 (1984).
90. A. M. Gabovich, D. P. Moiseev, L. V. Prokopovich, S. K. Uvarova, and V. E. Yachmenev, *Zh. Eksp. Teor. Fiz.* **86**, 1727 (1984).
91. D. P. Moiseev, S. K. Uvarova, and M. B. Fenik, *Fiz. Tverd. Tela* **23**, 2347 (1981).
92. S. Tajima, S. Uchida, A. Masaki, H. Takagi, K. Kitazawa, S. Tanaka, and A. Katsui, *Phys. Rev.* **B32**, 6302 (1985).
93. P. Szabó, P. Samuely, A. G. M. Jansen, P. Wyder, J. Marcus, T. Klein, and C. Escribe-Filippini, *J. Low Temp. Phys.* **106**, 291 (1997).
94. Z. Schlesinger, R. T. Collins, B. A. Scott, and J. A. Calise, *Phys. Rev.* **B38**, 9284 (1988).
95. M. Suzuki, Y. Enomoto, and T. Murakami, *J. Appl. Phys.* **56**, 2083 (1984).
96. C. U. Jung, J. H. Kong, B. H. Park, T. W. Noh, and E. J. Choi, *Phys. Rev.* **B59**, 8869 (1999).
97. V. N. Stepankin, A. V. Kuznetsov, E. A. Protasov, and S. V. Zaitsev-Zotov, *Pis'ma Zh. Eksp. Teor. Fiz.* **41**, 23 (1985).
98. T. H. Lin, X. Y. Shao, J. H. Lin, C. W. Chu, T. Inamura, and T. Murakami, *Solid State Commun.* **51**, 75 (1984).
99. S. Tomić, D. Jérôme, P. Monod, and K. Bechgaard, *J. Phys. (Paris) Lett.* **43**, L839 (1982).
100. T. Takahashi, D. Jérôme, and K. Bechgaard, *J. Phys. (Paris) Lett.* **43**, L565 (1982).
101. P. Garoche, R. Brusetti, and K. Bechgaard, *Phys. Rev. Lett.* **49**, 1346 (1982).
102. P. Garoche, R. Brusetti, D. Jérôme, and K. Bechgaard, *J. Phys. (Paris) Lett.* **43**, L147 (1982).
103. V. Vescoli, L. Degiorgi, B. Alavi, and G. Grüner, *Physica* **B244**, 121 (1998).

104. N. Cao, T. Timusk, and K. Bechgaard, *J. Phys. I (Paris)* **6**, 1719 (1996).
105. S. Belin and K. Behnia, *Phys. Rev. Lett.* **79**, 2125 (1997).
106. S. Belin, K. Behnia, and A. Deluzet, *Phys. Rev. Lett.* **81**, 4728 (1998).
107. H. Mori, *Int. J. Mod. Phys. B* **8**, 1 (1994).
108. L. Degiorgi, M. Dressel, A. Schwartz, B. Alavi, and G. Grüner, *Phys. Rev. Lett.* **76**, 3838 (1996).
109. Yu. G. Naidyuk and I. K. Yanson, *J. Phys.: Condens. Matter* **10**, 8905 (1998).
110. L. N. Bulaevskii, A. I. Buzdin, M.-L. Kulić, and S. V. Panjukov, *Adv. Phys.* **34**, 175 (1985).
111. L. E. De Long and K. A. Gschneidner, Jr., *Physica* **B163**, 158 (1990).
112. T. M. Palstra, A. A. Menovsky, J. van den Berg, A. J. Dirkmaat, P. H. Kess, G. J. Nieuwenhuys, and J. A. Mydosh, *Phys. Rev. Lett.* **55**, 2727 (1985).
113. M. B. Maple, J. W. Chen, Y. Dalichaouch, T. Kohara, C. Rossel, M. S. Torikachvili, M. W. McElfresh, and J. D. Thompson, *Phys. Rev. Lett.* **56**, 185 (1986).
114. N. H. van Dijk, F. Bourdarot, J. C. P. Klaasse, I. H. Hagmusa, E. Brück, and A. A. Menovsky, *Phys. Rev.* **B56**, 14493 (1997).
115. R. Escudero, F. Morales, and P. Lejay, *Phys. Rev.* **B49**, 15271 (1994).
116. S. A. M. Mentink, U. Wyder, J. A. A. J. Perenboom, A. de Visser, A. A. Menovsky, G. J. Nieuwenhuys, J. A. Mydosh, and T. E. Mason, *Physica* **B230–232**, 74 (1997).
117. E. A. Knetsch, J. J. Petersen, A. A. Menovsky, M. W. Meisel, G. J. Nieuwenhuys, and J. A. Mydosh, *Europhys. Lett.* **19**, 637 (1992).
118. A. Nowack, Yu. G. Naidyuk, P. N. Chubov, I. K. Yanson, and A. Menovsky, *Z. Phys.* **B88**, 295 (1992).
119. Yu. G. Naidyuk, O. E. Kvitnitskaya, A. Nowack, I. K. Yanson, and A. A. Menovsky, *Fiz. Nizk. Temp.* **21**, 310 (1995).
120. J. Aarts, A. P. Volodin, A. A. Menovsky, G. J. Nieuwenhuys, and J. A. Mydosh, *Europhys. Lett.* **26**, 203 (1994).
121. K. Hasselbach, J. R. Kirtley, and P. Lejay, *Phys. Rev.* **B46**, 5826 (1992).
122. P. Samuely, M. Kupka, K. Flachbart, and P. Diko, *Physica* **B206–207**, 612 (1995).
123. Y. DeWilde, J. Heil, A. G. M. Jansen, P. Wyder, R. Deltour, W. Assmuss, A. A. Menovsky, W. Sun, and L. Taillefer, *Phys. Rev. Lett.* **72**, 2278 (1994).
124. Yu. G. Naidyuk, H. von Löhneysen, G. Goll, I. K. Yanson, and A. A. Menovsky, *Europhys. Lett.* **33**, 557 (1996).
125. Yu. G. Naidyuk, K. Gloos, and A. A. Menovsky, *J. Phys.: Condens. Matter* **9**, 6279 (1997).
126. K. Matsuda, Y. Kohori, and T. Kohara, *Physica* **B230–232**, 351 (1997).
127. I. Felner and I. Nowik, *Solid State Commun.* **47**, 831 (1983).
128. C. Geibel, S. Thies, D. Kaczorowski, A. Mehner, A. Grauel, B. Seidel, U. Ahlheim, R. Helfrich, K. Petersen, C. D. Bredl, and F. Steglich, *Z. Phys.* **B83**, 305 (1991).
129. S. Süllo, B. Ludolph, B. Becker, G. J. Nieuwenhuys, A. A. Menovsky, and J. A. Mydosh, *Phys. Rev.* **B56**, 846 (1997).
130. M. Jourdan, M. Huth, P. Haibach, and H. Adrian, *Physica* **B259–261**, 621 (1999).
131. O. E. Kvitnitskaya, Yu. G. Naidyuk, A. Nowack, K. Gloos, C. Geibel, A. G. M. Jansen, and P. Wyder, *Physica* **B259–261**, 638 (1999).
132. Y. Nishihara, Y. Yamaguchi, T. Kohara, and M. Tokumoto, *Phys. Rev.* **B31**, 5775 (1985).
133. T. Nakama, M. Hedo, T. Maekawa, M. Higa, R. Resel, H. Sugawara, R. Settai, Y. Onuki, and K. Yagasaki, *J. Phys. Soc. Jpn.* **64**, 1471 (1995).
134. T. Ekino, H. Fujii, T. Nakama, and K. Yagasaki, *Phys. Rev.* **B56**, 7851 (1997).
135. Yu. G. Naidyuk, A. V. Moskalenko, I. K. Yanson, and C. Geibel, *Fiz. Nizk. Temp.* **24**, 495 (1998).
136. I. K. Yanson, in: *Symmetry and Pairing in Superconductors*, M. Ausloos and S. Kruchinin (eds.), Kluwer Academic, Dordrecht (1999), p. 271.
137. K. Murata, M. Ishibashi, Y. Honda, M. Tokumoto, N. Kinoshita, and H. Anzai, *J. Phys. Soc. Jpn.* **58**, 3469 (1989).
138. N. A. Fortune, K. Murata, K. Ikeda, and T. Takahashi, *Phys. Rev. Lett.* **68**, 2933 (1992).
139. A. Guillaume, B. Salce, J. Flouquet, and P. Lejay, *Physica* **B259–261**, 652 (1999).
140. T. Honma, Y. Haga, E. Yamamoto, N. Metoki, Y. Koike, H. Ohkuni, and Y. Onuki, *Physica* **B259–261**, 646 (1999).
141. G. Zwicknagl, *Adv. Phys.* **41**, 203 (1992).
142. A. M. Gabovich and A. I. Voitenko, *Fiz. Nizk. Temp.* **25**, 677 (1999).
143. F. Steglich, U. Ahlheim, A. Böhm, C. D. Bredl, R. Caspary, C. Geibel, A. Grauel, R. Helfrich, R. Köhler, M. Lang, A. Menher, R. Modler, C. Schank, C. Wassilew, G. Weber, W. Assmuss, N. Sato, and T. Komatsubara, *Physica* **C185–189**, 379 (1991).
144. H. Matsui, T. Goto, N. Sato, and T. Komatsubara, *Physica* **B199–200**, 140 (1994).
145. R. Modler, M. Lang, C. Geibel, C. Schank, and F. Steglich, *Physica* **B199–200**, 145 (1994).
146. R. Feyerherm, A. Amato, F. N. Gygax, A. Schenk, C. Geibel, F. Steglich, N. Sato, and T. Komatsubara, *Phys. Rev. Lett.* **73**, 1849 (1994).
147. R. Caspary, P. Hellmann, M. Keller, G. Sparr, C. Wassilew, R. Köhler, C. Geibel, C. Schank, and F. Steglich, *Phys. Rev. Lett.* **71**, 2146 (1993).
148. Y. Dalichaouch, M. C. de Andrade, and M. B. Maple, *Phys. Rev.* **B46**, 8671 (1992).
149. K. Matsuda, Y. Kohori, and T. Kohara, *Physica* **B259–261**, 640 (1999).
150. S. Murayama, C. Sekine, A. Yokoyanagi, K. Hoshi, and Y. Onuki, *Phys. Rev.* **B56**, 11092 (1997).
151. Y. Miyako, S. Kawarazaki, T. Taniguchi, T. Takeuchi, K. Marumoto, R. Hamada, Y. Yamamoto, M. Sato, Y. Tabata, H. Tanabe, M. Ocio, P. Pari, and J. Hammann, *Physica* **B230–232**, 1011 (1997).
152. M. Bullock, J. Zarestky, C. Stassis, A. Goldman, P. Canfield, Z. Honda, G. Shirane, and S. M. Shapiro, *Phys. Rev.* **B57**, 7916 (1998).
153. P. Dervenagas, J. Zarestky, C. Stassis, A. I. Goldman, P. C. Canfield, and B. K. Cho, *Phys. Rev.* **B53**, 8506 (1996).
154. S. K. Sinha, J. W. Lynn, T. E. Gregereit, Z. Hossain, L. C. Gupta, R. Nagarajan, and C. Godart, *Phys. Rev.* **B51**, 681 (1995).
155. T. Vogt, A. Goldman, B. Sternlieb, and C. Stassis, *Phys. Rev. Lett.* **75**, 2628 (1995).
156. C. Detlefs, A. I. Goldman, C. Stassis, P. Canfield, B. K. Cho, J. P. Hill, and D. Gibbs, *Phys. Rev.* **B53**, 6355 (1996).
157. K. Mizuno, T. Saito, H. Fudo, K. Koyama, K. Endo, and H. Deguchi, *Physica* **B259–261**, 594 (1999).
158. M. Nohara, M. Isshiki, H. Takagi, and R. J. Cava, *J. Phys. Soc. Jpn.* **66**, 1888 (1997).

159. M. Lang, M. Kürsch, A. Grauel, C. Geibel, F. Steglich, H. Rietschel, T. Wolf, Y. Hidaka, K. Kumagai, Y. Maeno, and T. Fujita, *Phys. Rev. Lett.* **69**, 482 (1992).
160. M. Nohara, T. Suzuki, Y. Maeno, T. Fujita, I. Tanaka, and H. Kojima, *Phys. Rev. Lett.* **70**, 3447 (1993).
161. A. M. Gabovich, V. A. Medvedev, D. P. Moiseev, A. A. Motuz, A. F. Prikhot'ko, L. V. Prokopovich, A. V. Solodukhin, L. I. Khirunenko, V. K. Shinkarenko, A. S. Shpigel, and V. E. Yachmenev, *Fiz. Nizk. Temp.* **13**, 844 (1987).
162. S. V. Lubenets, V. D. Natsik, and L. S. Fomenko, *Fiz. Nizk. Temp.* **21**, 475 (1995).
163. L. R. Testardi, *Phys. Rev.* **B12**, 3849 (1975).
164. P. Bourges, in: *The Gap Symmetry and Fluctuations in High Temperature Superconductors*, J. Bok, G. Deutscher, D. Pavuna, and S. A. Wolf (eds.), Plenum Press, New York (1998), p. 357.
165. M. K. Crawford, R. L. Harlow, E. M. McCarron, S. W. Tozer, Q. Huang, D. E. Cox, and Q. Zhu, in: *High-T_c Superconductivity 1996: Ten Years after the Discovery*, E. Kaldis, E. Liarokapis, and K. A. Müller (eds.), Kluwer Academic, Dordrecht (1997), p. 281.
166. M.-H. Julien, F. Borsa, P. Carretta, M. Horvatić, C. Berthier, and C. T. Lin, *Phys. Rev. Lett.* **83**, 604 (1999).
167. J. L. Cohn, C. P. Popoviciu, Q. M. Lin, and C. W. Chu, *Phys. Rev.* **B59**, 3823 (1999).
168. E. L. Nagaev, *Usp. Fiz. Nauk* **166**, 833 (1996).
169. A. A. Gorbatsevich, Yu. V. Kopaev, and I. V. Tokatly, *Zh. Eksp. Teor. Fiz.* **101**, 971 (1992).
170. C. Castellani, C. Di Castro, and M. Grilli, *Phys. Rev. Lett.* **75**, 4650 (1995).
171. E. S. Božin, S. J. L. Billinge, and G. H. Kwei, *Physica* **B241–243**, 795 (1998).
172. Y. Koyama, Y. Wakabayashi, K. Ito, and Y. Inoue, *Phys. Rev.* **B51**, 9045 (1995).
173. J. G. Naeni, X. K. Chen, J. C. Irwin, M. Okuya, T. Kimura, and K. Kishio, *Phys. Rev.* **B59**, 9642 (1999).
174. J. G. Naeni, X. K. Chen, K. C. Hewitt, J. C. Irwin, T. P. Devereaux, M. Okuya, T. Kimura, and K. Kishio, *Phys. Rev.* **B57**, 11077 (1998).
175. A. Lanzara, N. L. Saini, M. Brunelli, A. Valletta, and A. Bianconi, *J. Supercond.* **10**, 319 (1997).
176. A. I. Golovashkin, V. A. Danilov, O. M. Ivanenko, K. V. Mitsen, and I. I. Perepechko, *Pis'ma Zh. Eksp. Teor. Fiz.* **46**, 273 (1987).
177. G. V. M. Williams, J. L. Tallon, J. W. Quilty, H.-J. Trodahl, and N. E. Flower, *Phys. Rev. Lett.* **80**, 377 (1998).
178. C. Bernhard, D. Munzar, A. Wittlin, W. König, A. Golnik, C. T. Lin, M. Kläser, Th. Wolf, G. Müller-Vogt, and M. Cardona, *Phys. Rev.* **B59**, 6631 (1999).
179. Y. Wang, H. Shen, M. Zhu, and J. Wu, *Solid State Commun.* **76**, 1273 (1990).
180. N. L. Saini, A. Lanzara, A. Bianconi, and H. Oyanagi, *Phys. Rev.* **B58**, 11768 (1998).
181. J. L. Tallon, *Phys. Rev.* **B58**, 5956 (1998).
182. H. Ding, J. C. Campuzano, M. R. Norman, M. Randeria, T. Yokoya, T. Takahashi, T. Takeuchi, T. Mochiku, K. Kadowaki, P. Guptasarma, and D. G. Hinks, *J. Phys. Chem. Sol.* **59**, 1888 (1998).
183. Z.-X. Shen and D. S. Dessau, *Phys. Rep.* **253**, 1 (1995).
184. B. O. Wells, Y. S. Lee, M. A. Kastner, R. J. Christianson, R. J. Birgeneau, K. Yamada, Y. Endoh, and G. Shirane, *Science* **277**, 1067 (1997).
185. P. Dai, H. A. Mook, and F. Doğan, *Phys. Rev. Lett.* **80**, 1738 (1998).
186. Y. S. Lee, R. J. Birgeneau, M. A. Kastner, Y. Endoh, S. Wakimoto, K. Yamada, R. W. Erwin, S.-H. Lee, and G. Shirane, *Phys. Rev.* **B60**, 3643 (1999).
187. N. L. Saini, J. Avila, M. C. Asensio, S. Tajima, G. D. Gu, N. Koshizuka, A. Lanzara, and A. Bianconi, *Phys. Rev.* **B57**, 11101 (1998).
188. N. L. Saini, A. Bianconi, A. Lanzara, J. Avila, M. C. Asensio, S. Tajima, G. D. Gu, and N. Koshizuka, *Phys. Rev. Lett.* **82**, 2619 (1999).
189. J. Mesot, M. R. Norman, H. Ding, and J. C. Campuzano, *Phys. Rev. Lett.* **82**, 2618 (1999).
190. T. Timusk and B. Statt, *Rep. Prog. Phys.* **62**, 61 (1999).
191. L. N. Bulaevskii, *Usp. Fiz. Nauk* **115**, 263 (1975).
192. A. A. Varlamov and M. Ausloos, in: *Fluctuation Phenomena in High Temperature Superconductors*, M. Ausloos and A. A. Varlamov (eds.), Kluwer Academic, Dordrecht (1997), p. 3.
193. R. A. Klemm, in: *Fluctuation Phenomena in High Temperature Superconductors*, M. Ausloos and A. A. Varlamov (eds.), Kluwer Academic, Dordrecht (1997), p. 377.
194. C. Berthier, M. H. Julien, M. Horvatić, and Y. Berthier, *J. Phys. I (Paris)* **6**, 2205 (1996).
195. G. Blumberg, M. V. Klein, K. Kadowaki, C. Kendziora, P. Guptasarma, and D. Hinks, *J. Phys. Chem. Sol.* **59**, 1932 (1998).
196. A. V. Puchkov, D. N. Basov, and T. Timusk, *J. Phys.: Condens. Matter* **8**, 10049 (1996).
197. A. Ino, T. Mizokawa, K. Kobayashi, A. Fujimori, T. Sasa-gawa, T. Kimura, K. Kishio, K. Tamasaku, H. Eisaki, and S. Uchida, *Phys. Rev. Lett.* **81**, 2124 (1998).
198. J. Mesot and A. Furrer, in: *Neutron Scattering in Layered Copper-Oxide Superconductors*, A. Furrer (ed.), Kluwer Academic, Dordrecht (1998), p. 335.
199. J. Demsar, B. Podobnik, V. V. Kabanov, Th. Wolf, and D. Mihailovic, *Phys. Rev. Lett.* **82**, 4918 (1999).
200. J. W. Loram, K. A. Mirza, J. R. Cooper, and J. L. Tallon, *Physica* **C282–287**, 1405 (1997).
201. J. C. Campuzano, H. Ding, M. R. Norman, and M. Randeria, *Physica* **B259–261**, 517 (1999).
202. Z. Konstantinovic, Z. Z. Li, and H. Raffy, *Physica* **B259–261**, 567 (1999).
203. J. Bobroff, H. Alloul, P. Mendels, V. Viallet, J.-F. Marucco, and D. Colson, *Phys. Rev. Lett.* **78**, 3757 (1997).
204. A. S. Alexandrov, *Physica* **C305**, 46 (1998).
205. A. M. Gabovich, *Fiz. Nizk. Temp.* **18**, 693 (1992).
206. R. A. Klemm, in: *High Temperature Superconductivity: Ten Years after Discovery*, S. M. Bose and K. B. Garg (eds.), Narosa Publishing House, New Delhi, India (1998), p. 179.
207. A. M. Gabovich and A. I. Voitenko, *J. Phys.: Condens. Matter* **9**, 3901 (1997).
208. A. M. Gabovich and A. I. Voitenko, in: *Symmetry and Pairing in Superconductors*, M. Ausloos and S. Kruchinin (eds.), Kluwer Academic, Dordrecht (1999), p. 187.
209. G. Varelogiannis and M. Peter, *Czech. J. Phys.* **46**, Suppl. S2, 1047 (1996).
210. V. Hizhnyakov and E. Sigmund, *Phys. Rev.* **B53**, 5163 (1996).
211. A. Nazarenko and E. Dagotto, *Phys. Rev.* **B53**, 2987 (1996).
212. E. Dagotto, A. Nazarenko, and M. Boninsegni, *Phys. Rev. Lett.* **73**, 728 (1994).
213. T. Holstein, *Ann. Phys.* **8**, 325 (1959).

214. A. M. Afanas'ev and Yu. Kagan, *Zh. Eksp. Teor. Fiz.* **43**, 1456 (1962).
215. M.-H. Whangbo, E. Canadell, P. Foury, and J.-P. Pouget, *Science* **252**, 96 (1991).
216. P. M. Chaikin and R. L. Greene, *Phys. Today* **39**, 24 (1986).
217. G.-H. Gweon, J. D. Denlinger, J. A. Clack, J. W. Allen, C. G. Olson, E. DiMasi, M. C. Aronson, B. Foran, and S. Lee, *Phys. Rev. Lett.* **81**, 886 (1998).
218. J. Dumas and C. Schlenker, *Int. J. Mod. Phys.* **B7**, 4045 (1993).
219. B. T. Geilikman, *Studies in Low Temperature Physics*, Atomizdat, Moscow (1979), in Russian.
220. A. M. Gabovich and E. A. Pashitskii, *Fiz. Tverd. Tela* **20**, 761 (1978).
221. S. N. Artemenko and A. F. Volkov, *Zh. Eksp. Teor. Fiz.* **87**, 691 (1984).
222. A. A. Gorbatsevich and Yu. V. Kopaev, in: *Superconductivity, Superdiamagnetism, Superfluidity*, V. L. Ginzburg (ed.), Mir, Moscow (1987), p. 175.
223. Y. Enomoto, M. Suzuki, T. Murakami, T. Inukai, and T. Inamura, *Jpn. J. Appl. Phys. Lett.* **20**, L661 (1981).
224. P. Brison, P. Lejay, A. Buzdin, and J. Flouquet, *Physica* **C229**, 79 (1994).
225. K. Machida and T. Matsubara, *J. Phys. Soc. Jpn.* **50**, 3231 (1981).
226. A. I. Voitenko, A. M. Gabovich, and A. S. Shpigel, *Fiz. Nizk. Temp.* **18**, 108 (1992).
227. C. E. Methfessel, A. R. Stewart, B. T. Matthias, and C. K. N. Patel, *Proc. Nat. Acad. Sci. USA* **77**, 6307 (1980).
228. S. Tanaka, K. Kitazawa, and T. Tani, *Annual Rep. Eng. Res. Inst. Fac.: Eng. Univ. Tokyo* **41**, 131 (1982).
229. M. Sato, H. Fujishita, and S. Hoshino, *J. Phys.* **C16**, L417 (1983).
230. S. E. Stupp, M. E. Reeves, D. M. Ginsberg, D. G. Hinks, B. Dabrowski, and K. G. Vandervoort, *Phys. Rev.* **B40**, 10878 (1989).
231. J. E. Graebner, L. F. Schneemeyer, and J. K. Thomas, *Phys. Rev.* **B39**, 9682 (1989).
232. W. T. Kwok, U. Welp, G. W. Grabtree, K. G. Vandervoort, R. Hulscher, B. Dabrowski, and D. G. Hinks, *Phys. Rev.* **B40**, 9400 (1989).
233. P. Kumar, D. Hall, and R. G. Goodrich, *Phys. Rev. Lett.* **82**, 4532 (1999).
234. J. M. Heintz, M. Drillon, R. Kuentzler, Y. Dossmann, J. P. Kappler, O. Durmeyer, and F. Gautier, *Z. Phys.* **B76**, 303 (1989).
235. A. Junod, A. Erb, and C. Renner, *Physica* **C317-318**, 333 (1999).
236. M. N. Khlopkin, G. Kh. Panova, N. A. Chernoplekov, A. A. Shikov, and A. V. Suetin, *Zh. Eksp. Teor. Fiz.* **112**, 1386 (1997).
237. K. A. Moler, D. L. Sisson, J. S. Urbach, M. R. Beasley, A. Kapitulnik, D. J. Baar, R. Liang, and W. N. Hardy, *Phys. Rev.* **B55**, 3954 (1997).
238. K. N. Yang, M. B. Maple, L. E. De Long, J. G. Huber, and A. Junod, *Phys. Rev.* **B39**, 151 (1989).
239. A. D. Huxley, C. Paulsen, O. Laborde, J. L. Tholence, D. Sanchez, A. Junod, and R. Calemczuk, *J. Phys.: Condens. Matter* **5**, 7709 (1993).
240. G. Hilscher and H. Michor, in: *Quaternary Borocarbides, Superconductors and Hg-Based High-T_c Superconductors*, A. V. Narlikar (ed.), Nova Science, New York (1998).
241. S. Dorbolo, M. Houssa, and M. Ausloos, *Physica* **C267**, 24 (1996).
242. Yu. A. Izyumov and Yu. N. Skryabin, *Phys. Status Solidi* **B61**, 9 (1974).
243. G. B. Arnold, *Phys. Rev.* **B23**, 1171 (1981).
244. B. Keck and A. Schmid, *J. Low Temp. Phys.* **24**, 611 (1976).
245. L. V. Meisel and P. J. Cote, *Phys. Rev.* **B19**, 4514 (1979).
246. M. E. Palistrant and A. T. Trifan, *Theory of Impurity Superconductors under Pressure*, Shtiintsa, Kishinev (1980), in Russian.
247. A. S. Aleksandrov, V. F. Elesin, and N. P. Kazeko, *Fiz. Tverd. Tela* **21**, 2061 (1979).
248. P. Müller, H. Adrian, G. Ischenko, and H. Braun, *J. Phys. (Paris) Colloq.* **39**, C387 (1978).
249. S. V. Vonsovskii, Yu. A. Izyumov, and E. Z. Kurmaev, *Superconductivity of Transition Metals, Their Alloys and Compounds*, Nauka, Moscow (1977), in Russian.
250. H. Mutka, *Phys. Rev.* **B28**, 2855 (1983).
251. E. Helfand and N. R. Werthamer, *Phys. Rev.* **147**, 288 (1966).
252. R. V. Coleman and S. J. Hillenius, *Physica* **B105**, 428 (1981).
253. D. W. Youngner and R. A. Klemm, *Phys. Rev.* **B21**, 3890 (1980).
254. P. Entel and M. Peter, in: *Anisotropy Effects in Superconductivity*, Academic Press, New York (1977), p. 47.
255. M. Decroux, S. E. Lambert, M. S. Torikachvili, M. B. Maple, R. P. Guertin, L. D. Woolf, and R. Baillif, *Phys. Rev. Lett.* **52**, 1563 (1984).
256. R. A. Klemm, A. Luther, and M. R. Beasley, *Phys. Rev.* **B12**, 877 (1975).
257. L. N. Bulaevskii, O. V. Dolgov, and M. O. Ptitsyn, *Phys. Rev.* **B38**, 11290 (1988).
258. R. G. Dias and J. M. Wheatley, *Solid State Commun.* **98**, 859 (1996).
259. A. A. Abrikosov, *Phys. Rev.* **B56**, 5112 (1997).
260. S. Maekawa, H. Ebisawa, and H. Fukuyama, *J. Phys. Soc. Jpn.* **52**, 1352 (1983).
261. L. Coffey, K. Levin, and K. A. Muttalib, *Phys. Rev.* **B32**, 4382 (1985).
262. B. L. Altshuler and A. G. Aronov, *Zh. Eksp. Teor. Fiz.* **77**, 2028 (1979).
263. L. N. Bulaevskii and M. V. Sadovskii, *J. Low Temp. Phys.* **59**, 89 (1985).
264. K. Machida, K. Nokura, and T. Matsubara, *Phys. Rev.* **B22**, 2307 (1980).
265. K. Machida, T. Koyama, and T. Matsubara, *Phys. Rev.* **B23**, 99 (1981).
266. C. Ro and K. Levin, *Phys. Rev.* **B29**, 6155 (1984).
267. K. Kitazawa, A. Katsui, A. Toriumi, and S. Tanaka, *Solid State Commun.* **52**, 459 (1984).
268. S. V. Zaitsev-Zotov, A. V. Kuznetsov, E. A. Protasov, and V. N. Stepankin, *Fiz. Tverd. Tela* **26**, 3203 (1984).
269. I. O. Kulik, *Usp. Fiz. Nauk* **145**, 155 (1985).
270. C. Schlenker, H. Schwenk, C. Escribe-Filippini, and J. Marcus, *Physica* **B135**, 511 (1985).
271. M. Sato, Y. Matsuda, and H. Fukuyama, *J. Phys.* **C20**, L137 (1987).
272. V. F. Gantmakher, G. E. Tsyrynzhapov, L. P. Kozeeva, and A. N. Lavrov, *Zh. Eksp. Teor. Fiz.* **115**, 268 (1999).
273. D. D. Lawrie, J. P. Franck, J. R. Beamish, E. B. Molz, W.-M. Chen, and M. J. Graf, *J. Low Temp. Phys.* **107**, 491 (1997).
274. M. S. Osofsky, R. J. Soulen, Jr, S. A. Wolf, J. M. Broto, H. Rakoto, J. C. Ousset, G. Coffe, S. Askenazy, P. Pari,

- I. Bozovic, J. N. Eckstein, and G. F. Virshup, *Phys. Rev. Lett.* **71**, 2315 (1993).
275. A. P. Mackenzie, S. R. Julian, G. G. Lonzarich, A. Carington, S. D. Hughes, R. S. Liu, and D. C. Sinclair, *Phys. Rev. Lett.* **71**, 1238 (1993).
276. Y. Dalichaouch, B. W. Lee, C. L. Seamen, J. T. Markert, and M. B. Maple, *Phys. Rev. Lett.* **64**, 599 (1990).
277. E. H. Brandt, *Rep. Prog. Phys.* **58**, 1465 (1995).
278. D. E. Prober, R. E. Schwall, and M. R. Beasley, *Phys. Rev.* **B21**, 2717 (1980).
279. K. Onabe, M. Naito, and S. Tanaka, *J. Phys. Soc. Jpn.* **45**, 50 (1978).
280. M. Ikebe, K. Katagiri, K. Noto, and Y. Muto, *Physica* **B99**, 209 (1980).
281. J. L. Vicent, S. J. Hillenius, and R. V. Coleman, *Phys. Rev. Lett.* **44**, 892 (1980).
282. N. P. Ong, *Can. J. Phys.* **60**, 757 (1982).
283. M. S. Torikachvili and M. B. Maple, *Solid State Commun.* **40**, 1 (1981).
284. C. Y. Huang, D. W. Harrison, S. A. Wolf, W. W. Fuller, H. L. Luo, and S. Maekawa, *Phys. Rev.* **B26**, 1442 (1982).
285. W. M. Miller and D. M. Ginsberg, *Phys. Rev.* **B28**, 3765 (1983).
286. H. W. Meul, C. Rossel, M. Decroux, Ø. Fischer, G. Remenyi, and A. Briggs, *Phys. Rev. Lett.* **53**, 497 (1984).
287. L. E. De Long, J. G. Huber, K. N. Yang, and M. B. Maple, *Phys. Rev. Lett.* **51**, 312 (1983).
288. B. Damaschke and W. Felsch, *Z. Phys.* **63**, 179 (1986).
289. M. Tokumoto, K. Murata, H. Bando, H. Anzai, G. Saito, K. Kajimura, and T. Ishiguro, *Solid State Commun.* **54**, 1031 (1985).
290. D. U. Gubser, W. W. Fuller, T. O. Poehler, D. O. Cowan, M. Lee, R. S. Potember, L. Chiang, and A. N. Bloch, *Phys. Rev.* **B24**, 478 (1981).
291. I. J. Lee, M. J. Naughton, G. M. Danner, and P. M. Chaikin, *Phys. Rev. Lett.* **78**, 3555 (1997).
292. R. Brusetti, M. Ribault, D. Jérôme, and K. Bechgaard, *J. Phys. (Paris)* **43**, 801 (1982).
293. A. M. Gabovich and A. I. Voitenko, *Phys. Rev.* **B55**, 1081 (1997).
294. A. M. Gabovich and A. I. Voitenko, *Physica C* (1999), **239**, 198 (2000).
295. A. I. Larkin and Yu. N. Ovchinnikov, *Zh. Eksp. Teor. Fiz.* **51**, 1535 (1966).
296. A. Barone and G. Paterno, *The Physics and Applications of the Josephson Effect*, John Wiley and Sons, New York (1982).
297. A. M. Gabovich, E. A. Pashitskii, and A. S. Shpigel, *Fiz. Tverd. Tela* **18**, 3279 (1976).
298. X.-Z. Huang and K. Maki, *Phys. Rev.* **B46**, 162 (1992).
299. J. E. Hirsch, *Phys. Rev.* **B59**, 11962 (1999).
300. G. A. Levin and K. F. Quader, *Phys. Rev.* **B48**, 16184 (1993).
301. J. Y. T. Wei, C. C. Tsuei, P. J. M. van Bentum, Q. Xiong, C. W. Chu, and M. K. Wu, *Phys. Rev.* **B57**, 3650 (1998).
302. G. G. Melkonian and S. G. Rubin, *Phys. Rev.* **B57**, 10867 (1998).
303. A. M. Gabovich and A. I. Voitenko, *Phys. Rev.* **B56**, 7785 (1997).
304. T. Ekino and J. Akimitsu, *J. Phys. Soc. Jpn.* **58**, 2135 (1989).
305. M. Suzuki, K. Komoriota, H. Nakano, and L. Rinderer, *J. Less-Common Met.* **164–165**, 1579 (1990).
306. C. T. Jacobsen and M. T. Levinsen, *J. Less-Common Met.* **164–165**, 1550 (1990).
307. F. Morales, R. Escudero, D. G. Hinks, and Y. Zheng, *Physica* **C169**, 294 (1990).
308. T. Yamamoto, S. Suzuki, K. Takahashi, and Y. Yoshisato, *Physica* **C263**, 530 (1996).
309. J. R. Kirtley, *Int. J. Mod. Phys.* **B4**, 201 (1990).
310. I. K. Yanson, *Fiz. Nizk. Temp.* **17**, 275 (1991).
311. N. A. Belous, A. E. Chernyakhovskii, A. M. Gabovich, D. P. Moiseev, and V. M. Postnikov, *J. Phys.* **C21**, L153 (1988).
312. T. Ekino, T. Doukan, H. Fujii, F. Nakamura, S. Sakita, M. Kodama, and T. Fujita, *Physica* **C263**, 249 (1996).
313. G. T. Jeong, J. I. Kye, S. H. Chun, S. Lee, S. I. Lee, and Z. G. Khim, *Phys. Rev.* **B49**, 15416 (1994).
314. Ya. G. Ponomarev, B. A. Aminov, N. B. Brandt, M. Hein, C. S. Khi, V. Z. Kresin, G. Müller, H. Piel, K. Rosner, S. V. Tchesnokov, E. B. Tsokur, D. Wehler, R. Winzer, Th. Wolfe, A. V. Yarygin, and K. T. Yusupov, *Phys. Rev.* **B52**, 1352 (1995).
315. A. I. Akimenko, G. Goll, I. K. Yanson, H. V. Löhneysen, R. Ahrens, T. Wolf, and H. Wühl, in: *Abstracts of the 3rd USSR Symposium on High Temperature Superconductivity*, FTINT, Kharkov (1991), Vol. II, p. 85, in Russian.
316. T. Nakano, N. Momono, M. Oda, and M. Ido, *J. Phys. Soc. Jpn.* **67**, 2622 (1998).
317. Ch. Renner, B. Revaz, J.-Y. Genoud, K. Kadowaki, and Ø. Fischer, *Phys. Rev. Lett.* **80**, 149 (1998).
318. A. K. Gupta and K.-W. Ng, *Int. J. Mod. Phys.* **B12**, 3271 (1998).
319. M. Suzuki, S.-i. Karimoto, and K. Namekawa, *J. Phys. Soc. Jpn.* **67**, 732 (1998).
320. C. Manabe, M. Oda, and M. Ido, *J. Phys. Soc. Jpn.* **66**, 1776 (1997).
321. L. Ozyuzer, J. F. Zasadzinski, C. Kendziora, and K. E. Gray, *Phys. Rev.* **B61**, 3629 (1999).
322. A. Mourachkine, *Physica* **C323**, 137 (1999).
323. A. M. Cucolo and P. Prieto, *Int. J. Mod. Phys.* **B11**, 3833 (1997).
324. B. Barbiellini, Ø. Fischer, M. Peter, Ch. Renner, and M. Weger, *Physica* **C220**, 55 (1994).
325. T. Ekino, T. Doukan, and H. Fujii, *J. Low Temp. Phys.* **105**, 563 (1996).
326. S. Kashiwaya, T. Ito, K. Oku, S. Ueno, H. Takashima, M. Koyanagi, Y. Tanaka, and K. Kajimura, *Phys. Rev.* **B57**, 8680 (1998).
327. M. V. Eremin and I. A. Larionov, *Pis'ma Zh. Eksp. Teor. Fiz.* **68**, 611 (1998).
328. G. Varelogiannis, *Phys. Rev. Lett.* **76**, 3236 (1996).
329. S. H. Liu and R. A. Klemm, *Phys. Rev. Lett.* **73**, 1019 (1994).
330. J. Bok and J. Bouvier, *Physica* **C274**, 1 (1997).
331. D. Coffey and L. Coffey, *Phys. Rev. Lett.* **76**, 3237 (1996).
332. Ya. G. Ponomarev, E. B. Tsokur, M. V. Sudakova, S. N. Tchesnokov, M. E. Shabalin, M. A. Lorenz, M. A. Hein, G. Müller, H. Piel, and B. A. Aminov, *Solid State Commun.* **111**, 513 (1999).
333. K. Gloos, F. B. Andres, B. Buschinger, and C. Geibel, *Physica* **B230–232**, 391 (1997).